热烈庆祝中国地质学会成立100周年
1922～2022
www.geojournals.cn/georev

断层带中假玄武玻璃成因机制及非稳态流变意义

李文元，曹淑云
中国地质大学(武汉)地球科学学院，地质过程与矿产资源国家重点实验室，武汉，430074

内容提要：假玄武玻璃呈玻璃质或隐晶质特性，常常与断层带相伴出现，其形成能有效地降低断层摩擦强度，被认为是古地震快速滑动的化石纪录。因此，对假玄武玻璃的研究对深入了解深部就位的断层变形和地震成因机制等具有重要意义。尽管国内外学者对假玄武玻璃开展了长期的研究，也积累了丰富的资料，然而，由于天然假玄武玻璃非常少见或零星地被报道，再加上其形成环境和过程的复杂性，对假玄武玻璃的构造特征、形成环境和成因机制仍然存在诸多争议及亟待解决的关键科学问题。研究表明，假玄武玻璃可以发育在大陆岩石圈不同深度范围内，即中下地壳乃至上地幔以糜棱岩为主的韧性变形领域(>60 km)，或中上地壳层次以碎裂岩为主的脆性变形域(<12 km)。越来越多证据也显示出在断层带的脆—韧性转换域中形成的假玄武玻璃跟浅源地震活动直接关联，也意味着中上地壳脆性变形和中下地壳塑性变形之间存在着更为复杂的耦合关联，同时对不同深部岩石强度和力学行为提出了挑战。对假玄武玻璃形成机制存在由断层面上的摩擦热导致的摩擦熔融体或仅仅是断层面岩石超碎裂粉碎作用认识的争议。而有研究认为干的环境有利于假玄武玻璃形成，因为流体的存在会降低断层面的有效正应力，不利于热量的积累以及摩擦熔融的进行；然而，另外一种观点认为流体的存在可以降低矿物熔融温度有利于断层摩擦熔融及形成假玄武玻璃。本文从假玄武玻璃的形成机制、形成深度、流体影响、形成后对断层强度的影响、以及保存与破坏机制几方面进行了最新总结，并对假玄武玻璃中非晶态物质的成因、脆—韧性转换带之下岩石的变形机制以及对陆壳强度的影响和非稳态流变意义进行探讨。

关键词：假玄武玻璃、超碎裂—粉碎、摩擦熔融、断层弱化与强化、地震、流体作用

假玄武玻璃呈暗棕色、黑色玻璃质或隐晶质特性。岩石的外貌很像玻璃质火山熔岩中的玄武玻璃，故称为假玄武玻璃(Pseudotachylyte，也有写成Pseudotachylite)。其常常与断层带相伴出现，通常被认为是与地震断层有关的高应变速率条件下的产物，因此也被誉为“地震化石”。对假玄武玻璃的认识可追溯到19世纪初。MacCulloch(1819)用“暗色岩石(trap rock)”来描述沿苏格兰西部岛屿东侧太古宙片麻岩中分布的假玄武玻璃，并将这种暗色岩石描述为镶嵌在玄武岩中由片麻岩和花岗岩碎片组成的砾岩。Clough(1888)和Clough等(1909)分别将英格兰切维奥特山的花岗岩中和与苏格兰格伦科火山口沉陷有关的环形断层中发育的假玄武玻璃描述为“坚硬压碎岩(flinty crush rock)”。

假玄武玻璃这一术语是由Shand(1916)提出，用来描述南非Vredfort花岗岩群北部Parijs地区太古宙片麻岩中呈脉状或网脉状的暗色隐晶质岩石。这类岩石与玻状玄武岩相似，但其物理和化学成因明显不同，故称假玄武玻璃。之后，国内外学者对假玄武玻璃的类型、野外产状和形态分布、显微构造特征、地球化学、实验模拟等开展了不同程度的研究(e. g.，McKenzie and Brune，1972；Sibson，1975，1986；Wenk，1978；杨主恩等，1981；邵济安等，1988；Passchier，1982；Magloughlin，1992；Swanson，1992；Lin Aiming，1994a，b；张进江和郑亚东，1995；张桂林，1997；Cowan，1999；林爱明等，2002；刘建民等，2003，2005，2009；Rowe et al.，2005；Di Toro et al.，2006，2009；Spray，2010；Bestmann et al.，2011；Proctor and Lockner，2016；Hung Chiencheng et al.，2019)。国内学者们相继对新疆二台断裂带(史兰斌等，1997；刘建民，2009)、贺兰山地区(胡能高等，1995)、桐柏—大别造山带

注：本文为国家自然科学基金资助项目(编号：41972220、41722207)和国家重点研发计划项目(编号：SQ2017YFSF040030)的成果。
收稿日期：2021-09-06；改回日期：2022-01-04；网络首发：2022-01-20；责任编辑：刘志强。Doi：10.16509/j.georeview.2022.01.081
作者简介：李文元，男，1996年生，博士研究生，构造地质学、显微构造分析专业；Email：Wenyuanli@cug.edu.cn。通讯作者：曹淑云，女，1978年生，教授，长期从事区域构造地质和显微构造分析研究；shuyun.cao@cug.edu.cn。

(林爱明等,2002;刘建民等,2003,2004,2005)、嵩山登封大断层(侯广顺等,2013)、兰坪河西雪龙山岩群(沙绍礼和陈晓林,2013)、豫西双龙剪切带(靳立杰等,2014)、以及广东河台(张桂林和梁金城,1998;王历星等,2019)的假玄武玻开展了野外产状、化学成分、成因机制的研究,并探讨了同震断裂的破裂机制及地震学意义。

近年来,一些学者通过对龙门山断裂带中地表出露及钻孔岩芯中的假玄武玻璃开展研究,认为龙门山构造带形成演化过程中长期伴随有地震活动,这为认识汶川地震的发生机制提供了重要科学依据(Li Haibing et al., 2013; 王焕等,2013,2015;Wang Huan et al., 2015;Zheng Yong et al., 2016; 李海兵等, 2018; 张蕾等, 2017, 2019; Zhang Lei et al., 2021; Dang Jiaxiang et al., 2021)。然而,由于天然假玄武玻璃非常少见或仅零星存在不同地区,再加上其形成环境和过程的复杂性,对假玄武玻璃和相关岩石的构造特征、形成环境和成因机制等目前仍然存在争议,亟待持续开展深入的研究。下面对假玄武玻璃的形成环境、成因机制、流体(水)作用、对断层滑移的影响以及形成后的保存与破坏等几个方面分别进行了总结并对其地质意义进行了探讨。

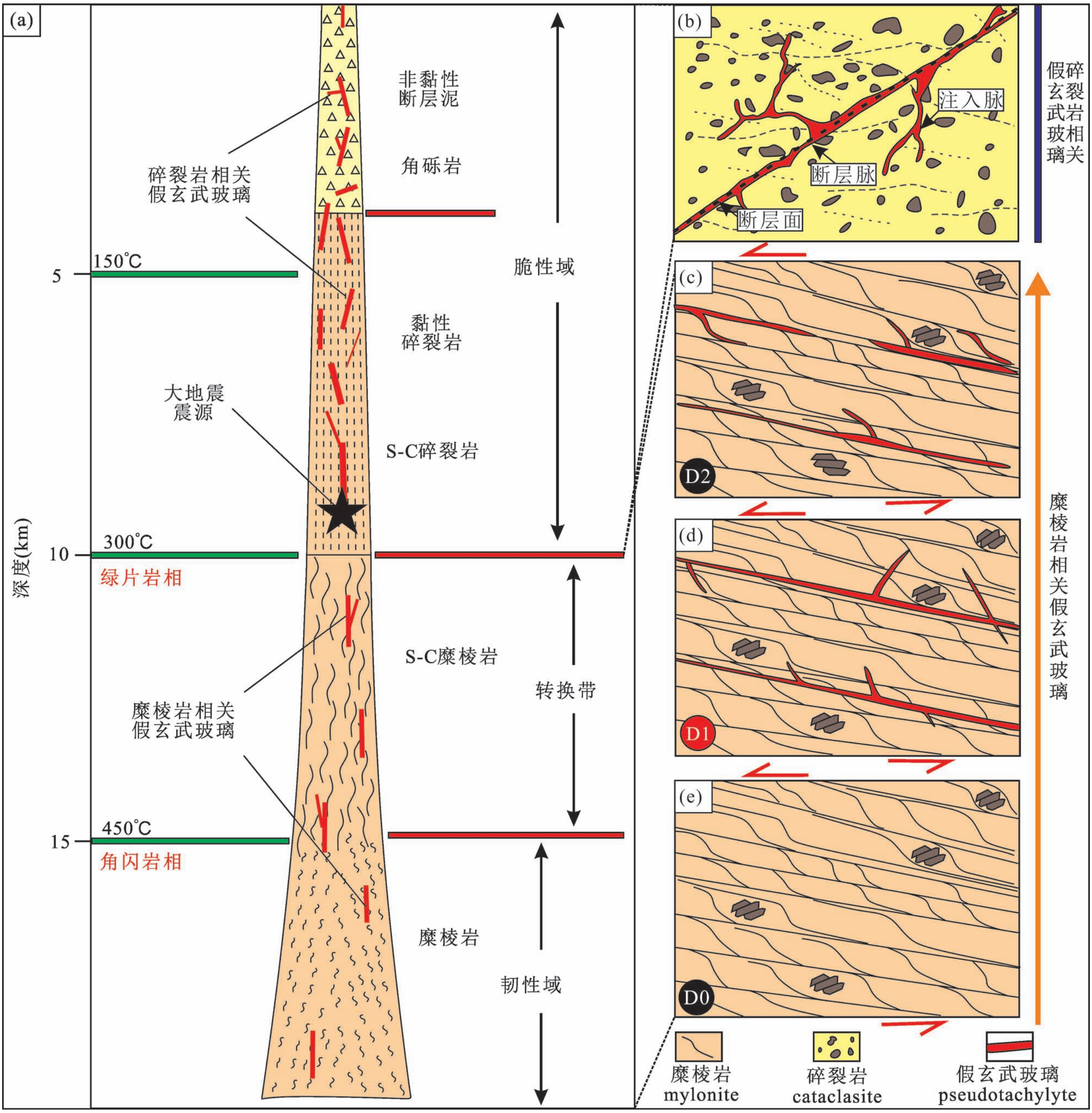

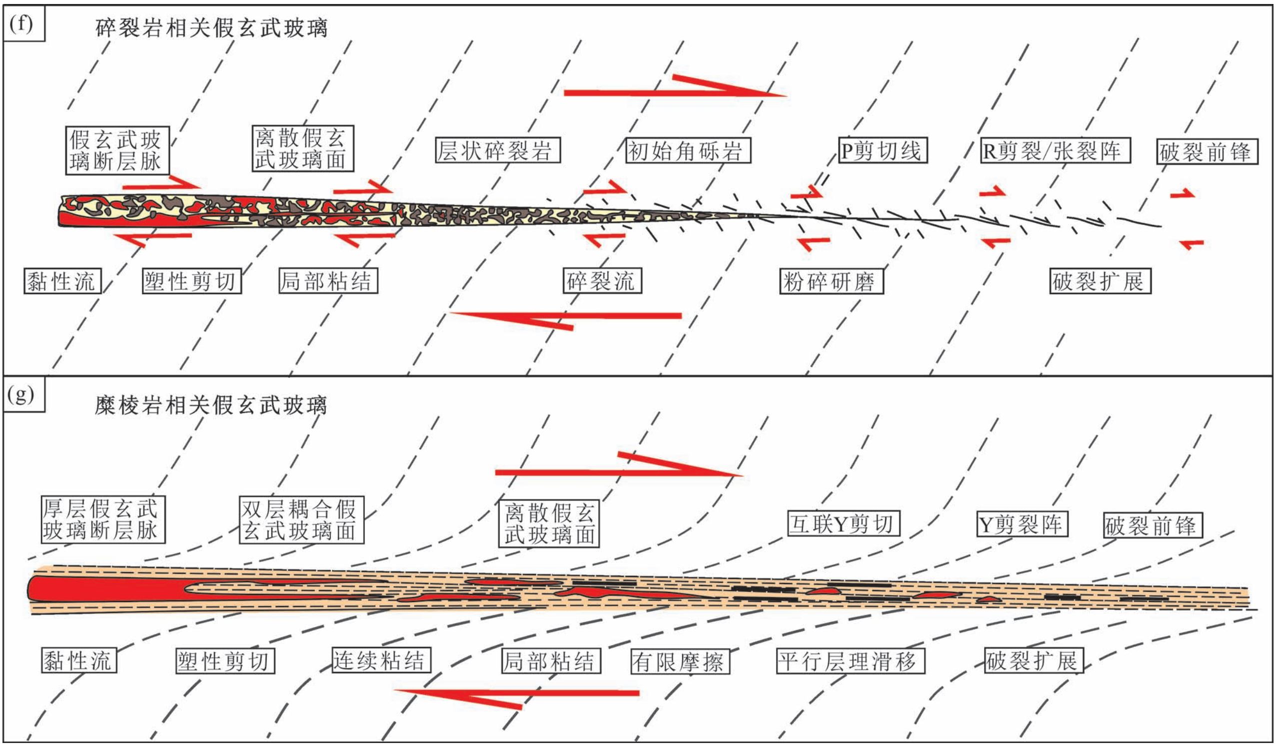

图 1 走滑孕震带构造剖面示意图(据 Swanson, 1992; Lin Aiming, 2008 修改)

Fig. 1 Structural profile of strike slip seismogenic belt (modified after Swanson, 1992; Lin Aiming, 2008)

(a)脆—韧性转变、变形和粉碎机制随地壳深度变化以及假玄武玻璃的分布。(b)碎裂岩相关假玄武玻璃产状示意图,假玄武玻璃与碎裂岩伴生,且通常切割岩石先存面理。(c)—(e)糜棱岩相关假玄武玻璃产状示意图:(c)假玄武玻璃形成后,在左行剪切作用下,假玄武玻璃发生变形—糜棱岩化;(d)地震破裂导致形成假玄武玻璃脉体,断层脉通常与围岩面理产状一致,注入脉以高角度切割围岩;(e)在深部韧性域中,岩石在左行剪切作用下发生塑性变形形成糜棱岩。(f)—(g)地震断层扩展演化空间模式(据 Swanson, 1992 修改):(f)上地壳以脆性破裂摩擦为主的摩擦熔融模式;以假玄武玻璃—碎裂岩组合为基础;(g)下地壳以韧性黏结摩擦为主的摩擦熔融模式,以假玄武玻璃—糜棱岩组合为基础

(a) Brittle—ductile transition, deformation and wear mechanisms change with crustal depth and the distribution of pseudotachylyte. (b) Formation of pseudotachylyte relates cataclastic rock usually cut the pre-existing foliation of rocks. (c)—(e) Formation of pseudotachylyte relates to mylonite: (c) pseudotachylyte was deformed to form mylonitic rock during left-lateral shearing; (d) seismic rupture leads to the formation of pseudotachylyte veins; fault veins are usually consistent with the occurrence of surrounding rock foliation, and the injection veins cut the surrounding rock at a high angle; (e) in the deep-seated ductile domain, the rock is plastically deformed under left lateral shearing to form mylonite. (f)—(g) Evolution of seismic fault propagation (modified according to Swanson, 1992): (f) friction melting mode of the upper crust is mainly brittle fracture friction by pseudotachylyte cataclastic rock assemblage; (g) friction melting mode of the lower crust is dominated by ductile adhesive friction by the pseudotachylyte mylonite assemblage

1 假玄武玻璃的形成环境

研究表明,假玄武玻璃可以形成于不同的构造环境中,如①陨石撞击所形成的冲击构造,如南非 Vredfort 地区中的假玄武玻璃(Martini, 1992; Spray, 1995),认为是在撞击点附近由于摩擦熔融或减压熔融形成的熔体快速冷却(Reimold, 1995; Melosh, 2005; French and Koeberl, 2010; Reimold et al., 2017);②断裂带的快速摩擦滑动,在断层面或大型滑坡面附近,由于岩层快速滑动,岩石在滑动面发生碎裂化作用或摩擦熔融(Sibson, 1986; Spray, 1992; Sibson and Toy, 2006; Lin Aiming, 2008; Di Toro et al., 2009; Bestmann et al., 2011)。尽管最早对于假玄武玻璃的研究是基于冲击构造展开的(Shand, 1916),但对假玄武玻璃的了解大部分来自于对断层的研究,其断层活动与地震过程紧密关联(Spray, 1995, 2010),因此,断层构造成因的假玄武玻璃通常被视为古地震活动的“化石”记录器(Sibson, 1975; Cowan, 1999; Rowe et al., 2005)。

基于野外观察和实验研究表明,假玄武玻璃的形成深度可分布在整个传统发震带(脆—韧性转换带及之上区域)甚至是韧性变形域(图 1a),记录了

发震源区以及剥露过程的重要信息,是联结实际地震破裂过程与地震成因理论的枢纽,对我们深入了解并探讨断裂发展过程、形成机制、地震活动脉动性、地震成因机制、预算地震能量、同震断层滑动的热历史具有重要启示意义(Sibson, 1975; Magloughlin, 1992; Di Toro et al., 2006, 2009)。虽然近些年对断裂系统的深入研究表明,一些其他的构造特征或指标也可记录同震滑动的信息(王焕和李海兵,2019),如脱挥发分结构(Han et al., 2007; Verberne et al., 2014)、有机质成熟度(Oohashi et al., 2011; Kuo Liwei et al., 2017)微量元素迁移特征(Ishikawa et al., 2008)、断层镜面构造(Kuo Liwei et al., 2016)、液化粒状流(Otsuki et al., 2003; Kirkpatrick and Shipton, 2009)、碎屑—皮层集合体(Boutareaud et al., 2008, 2010; Boullier et al., 2009)、同震晶体塑性变形(John et al., 2009; Kim et al., 2010)等,但事实上假玄武玻璃仍是识别古地震最直接最有效的标志,是研究古地震的最好媒介。

根据假玄武玻璃脉体与断层面产状关系(Sibson, 1975),可以将假玄武玻璃划分为断层脉(断层面上所形成的源脉)和注入脉(由断层面上所产生的熔体及细粒碎屑注入到围岩同震裂隙中所形成的单脉或网脉)(图 1b)。现有研究表明在地壳不同深度条件下均可产生假玄武玻璃(图 1a),不同深度产生的假玄武玻璃通常具有以下特点:①在脆性条件下形成的假玄武玻璃通常与碎裂岩伴生,假玄武玻璃通常切割岩石先存面理或层理,呈脉状或网脉状分布(图 1b)。②在韧性条件下形成的假玄武玻璃通常与糜棱岩伴生,在深部韧性域中,地震破裂通常沿薄弱面(如面理)进行传播,通常形成脉体形状相对简单且与围岩糜棱面理产状一致的假玄武玻璃,但注入脉通常以大角度切割围岩,当假玄武玻璃形成后,在后期剪切作用下假玄武玻璃发生塑性变形,导致脉体形态也受后期剪切变形控制(图 1c—e)。地震断层是沿破裂前锋发展的,造成不同深度假玄武玻璃产状差异的原因可能是破裂前锋的扩展方式不同,在浅部脆性域中,破裂前锋带形成 R 剪裂/张裂阵(图 1f),在深部韧性域中,破裂前锋带受先存糜棱面理影响,形成平行于剪切面的 Y 剪裂阵(图 1g)(张进江和郑亚东,1995)。

前人对假玄武玻璃的研究与争议多聚焦在以下方面:①假玄武玻璃的形成机制,摩擦熔融或超碎裂粉碎(Sibson, 1975; Wenk, 1978; Magloughlin, 1992; Spray, 1995; Ozawa and Takizawa, 2007; Pec et al., 2012b)。②流体在形成假玄武玻璃过程中的作用,无水断层 vs. 富水断层(Scholz et al., 1973; Magloughlin, 1992; Rowe et al., 2005; Ferrand et al., 2017; Brantut, 2020)。③假玄武玻璃形成对断层滑移的影响,润滑剂 vs. 黏性抑制剂(McKenzie and Brune, 1972; Tsutsumi and Shimamoto, 1997; Di Toro et al., 2004a, 2006; Niemeijer et al., 2011; Kendrick et al., 2014; Hayward and Cox, 2017; Wallace et al., 2019)。④在实验室中通过摩擦熔融实验,了解与断层有关的假玄武玻璃形成的力学机制和熔融过程,来反演地震活动期间断层的情况(McKenzie and Brune, 1972; Spray, 1995; Di Toro et al., 2006; Proctor and Lockner, 2016; Hung Chiencheng et al., 2019; Papa et al., 2021; Zhang Lei et al., 2021)。⑤通过理论和实验来计算产生假玄武玻璃所需要的能量和条件、震源参数、同震熔体压力等(Di Toro et al., 2006, 2009; Spray, 2010; Ferrand et al., 2018, 2021)。

2　假玄武玻璃成因机制和基本特征

对假玄武玻璃及相关岩石的形成机制争论的焦点主要集中在摩擦熔融成因(melting-originated pseudotachylyte)(Sibson, 1975, 1980; Magloughlin, 1992; Spray, 2010),还是摩擦粉碎/超碎裂作用(crushing-originated pseudotachylyte)(Wenk, 1978; Weiss and Wenk, 1983; Janssen et al., 2010)。

2.1　摩擦熔融成因

断层面摩擦加热导致矿物发生熔融,产生的熔体冷却后同残存的碎屑一起形成假玄武玻璃这一成因机制被学者所广泛接受(Holland, 1900; Clough et al.,1909; Shand, 1916; Sibson, 1975; Magloughlin 1992)。摩擦熔融是极端应变局部化的一种表现,通常被认为是在应变速率>10^{-2} s^{-1} 和滑移速率>0.1 m/s(Spray, 1992)。野外宏观特征、显微构造特征以及岩相学证据(Sibson, 1975; Maddock, 1983; Maddock et al., 1987; Lin Aiming, 1991, 1994a, b; Ikesawa et al., 2003; Di Toro and Pennacchioni, 2005; Rowe et al., 2005; Bestmann et al., 2011; Rowe et al., 2012; 王焕等, 2015),并结合摩擦熔融实验表明在一定深度范围可以通过摩擦加热导致矿物熔融产生假玄武玻璃(McKenzie and Brune, 1972; Spray, 1995; Tsutsumi and Shimamoto, 1997; Lin Aiming and Shimamoto, 1998; Di Toro et al., 2006; Niemeijer et al., 2011; Kendrick et al., 2014; Hornby et al., 2015; Proctor and Lockner, 2016; Wallace et al., 2019)。

熔融成因假玄武玻璃的典型标志包括有:①由基质和碎屑两部分组成,多以黑褐—灰黄—黄褐色脉状或者网脉状产出,穿插在断层带的岩石中,有时可以识别出多期假玄武玻璃脉体(年轻脉体切割并覆盖了较老的脉体),不同期次假玄武玻璃脉体之间的接触边界一般比较尖锐(图 2)。②基质主要由致密隐晶质—玻璃质物质组成(图 2c, f, g)(Toyoshima, 1990; Lin Aiming, 1994a),且有时可见不同形状的且只有高温和快速淬火条件下形成的微晶或者球晶(图 2j)(Maddock, 1983; Lin Aiming, 1994b; Di Toro and Pennacchioni, 2004; Wang Huan et al., 2019);③存在气泡和杏仁体(Maddock et al., 1987);④流动状构造(图 2g)(Di Toro et al., 2009);⑤淬火的硫化物熔滴(Magloughlin, 1992, 2005);⑥碎屑主要由大小不等(一般小于 0.2

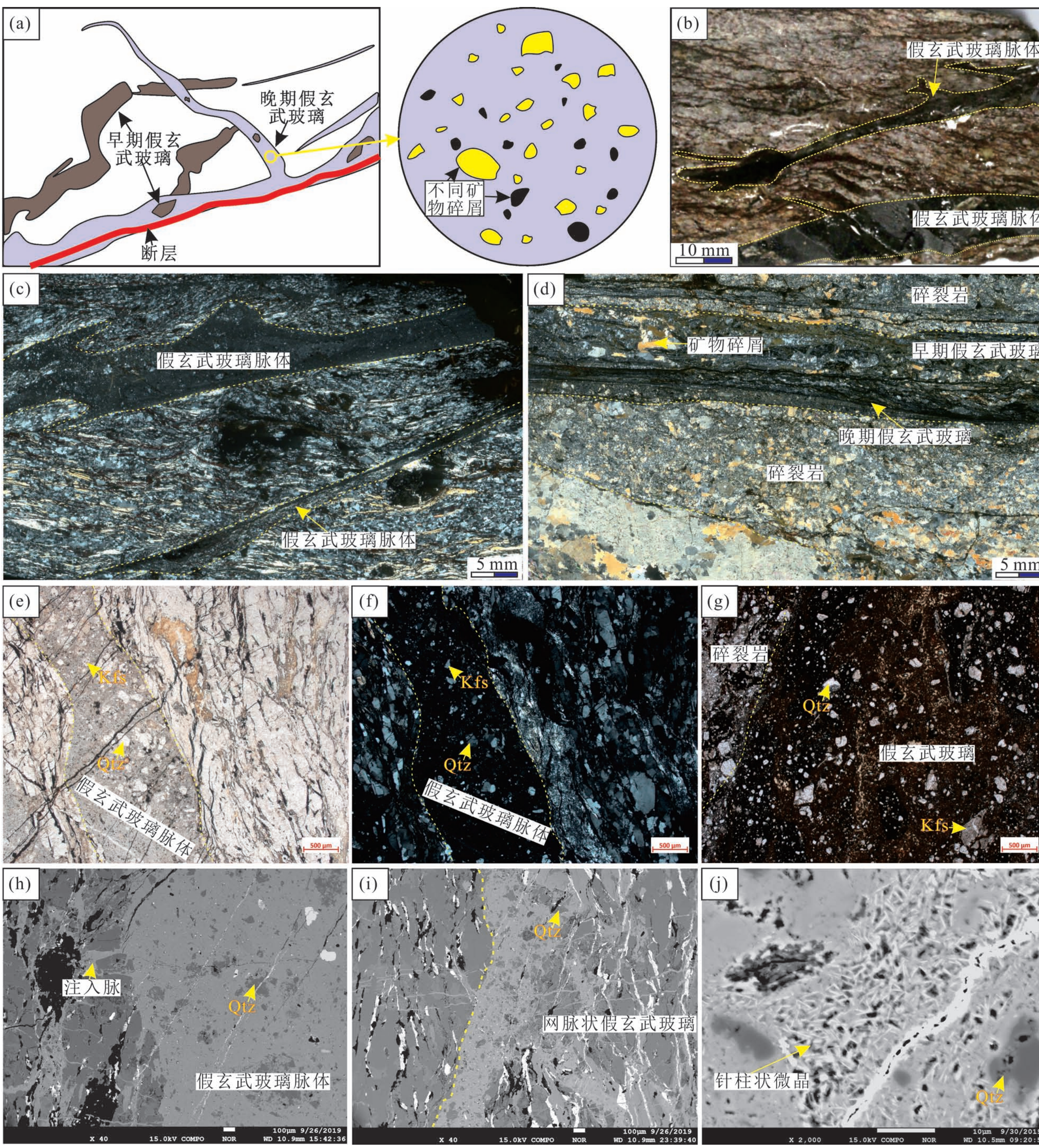

图 2 假玄武玻璃宏观—显微构造特征

Fig. 2 Macroscopic and microscopic structural characteristics of pseudotachylyte

(a)不同期次假玄武玻璃脉交切关系示意图；(b)假玄武玻璃及围岩宏观手标本照片；(c)假玄武玻璃脉体斜切围岩糜棱面理显微照片；(d)不同期次假玄武玻璃脉体显微照片，假玄武玻璃脉体周围伴生有碎裂岩；(e)—(f)假玄武玻璃脉体显微照片，基质呈玻璃质—隐晶质，脉体中含有石英碎屑；(g)与碎裂岩伴生的假玄武玻璃显微照片，碎屑成分主要由长石和石英，具有流动结构；(h)假玄武玻璃与围岩接触边界 BSE 图像，假玄武玻璃注入到围岩裂隙中；(i)网脉状假玄武玻璃 BSE 图像；(j)假玄武玻璃基质中针柱状微晶 BSE 图像；所有样品采自东阿尔卑斯山 Mur—Mürz 断层带

(a) Cross cutting relationship of pseudotachylyte veins in different stages; (b) macro hand specimens of pseudotachylyte and surrounding rock; (c) micrograph of mylonite foliation of oblique cut surrounding rock of pseudotachylyte vein; (d) micrograph of pseudotachylyte veins at different stages show that cataclastic rocks are associated around pseudotachylyte veins; (e)—(f) micrograph of pseudotachylyte vein, the matrix is glassy cryptocrystalline, and the vein contains quartz clasts; (g) micrographs of pseudotachylyte associated with cataclastic rocks; the clastic components are mainly feldspar and quartz, with flow structure; (h) BSE image of the contact boundary between pseudotachylyte and surrounding rock, and pseudotachylyte is injected into the cracks of surrounding rock; (i) BSE image of reticulated pseudotachylyte; (j) BSE image of needle columnar microcrystals in pseudotachylyte matrix. All samples were taken from the Mur—Mürzfault zone in the eastern Alps

mm)，圆—次圆状的石英、长石颗粒组成(图 2e—i)；⑦由矿物选择性熔融导致的假玄武玻璃与母岩某些化学成分的系统性变化(Maddock, 1992; Magloughlin and Spray, 1992; Lin Aiming and Shimamoto, 1998)；以及一些其他的证据如港湾状的碎屑、冷凝/淬火边(Philpotts, 1964; Lin Aiming, 1994a)、以及碎屑的圆度(>0.4)(Lin Aiming, 1999)、高磁化率值或高剩磁强度特征(张蕾等, 2019)。

化学成分分析表明，熔融成因假玄武玻璃脉整体化学成分从基性到酸性各不相同，但假玄武玻璃全岩(基质+碎屑)的主要化学成分与其母岩类似，而且稀土元素和微量元素总体含量也变化不大，说明假玄武玻璃是母岩原地熔融而成的(Wenk et al., 1982; Magloughlin, 1989, 1992; Lin Aiming, 1994a, b; Lin Aiming and Shimamoto, 1998)。而假玄武玻璃基质的化学成分与母岩有较为显著的差异。如基质中 SiO_2 含量相对较低，而 Al_2O_3、FeO、MgO、TiO_2 的含量则相对偏高，K、Ca、Na 具有不稳定性(Lin Aiming, 1994a; Lin Aiming and Shimamoto, 1998; Di Toro and Pennacchioni, 2005; Wang Huan et al., 2019; 王历星等, 2019)。学者们认为这种化学成分的改变是由母岩中含水矿物和镁铁质矿物(如云母、角闪石等，具有相对较低的单相熔点且伴随 H_2O 的释放)的选择性熔融引起的(O'Hara, 1992; Jiang Hehe et al., 2015; Wallace et al., 2019)。最初学者们认为摩擦熔融过程是化学平衡过程，但平衡熔融需要足够长的时间来完成不同矿物相之间的所有化学反应，而假玄武玻璃熔体的产生到冷却是一个快速的过程(与假玄武玻璃生成有关的地震滑动事件被认为在几秒或更短的时间尺度上发生)。随着研究的深入，发现熔融成因的假玄武玻璃中残留的矿物碎屑多是石英、长石，而云母、角闪石这类含水的镁铁质矿物含量很少，不符合平衡熔融的特征。现在学者们已经从实验和理论上证明，假玄武玻璃形成过程是一种非平衡绝热熔融过程，涉及单个矿物相按照固相线温度选择性熔融，而不是全岩平衡熔融(Allen, 1979; Maddock, 1992; Magloughlin, 1992; Lin Aiming, 1994a; Lin Aiming and Shimamoto, 1998; Di Toro and Pennacchioni, 2004; Spray, 2010; Wang Huan et al., 2019)。在一定程度上可以用摩擦熔体的成分演化来约束源区性质和滑动持续时间(Jiang Hehe et al., 2015)。在假玄武玻璃形成过程中，常见矿物的熔融顺序一般是：云母(约 650℃)、角闪石(约 750～850℃)、辉石(约 800～1425℃)、长石(约 1100～1555℃)、石英(约 1700～1730℃)(Spray, 2010)。

2.2　超碎裂成因

超碎裂—粉碎作用是形成假玄武玻璃的另一种重要机制(Clough, 1888; Wenk, 1978; Ozawa and Takizawa, 2007; Pec et al, 2012b)。超碎裂成因假玄武玻璃在宏观露头与微观显微尺度上表现出与熔融成因假玄武玻璃相似的特征，也可以呈脉状或者网脉状形式出现(图 3a—c)，在普通光学显微镜下也是由碎屑和隐晶质的基质组成(图 3d)，甚至也可见流动状构造(图 3e)(Ozawa and Takizawa, 2007; 靳立杰等, 2014)。在更高放大倍数的电子显微镜下可以发现碎裂成因的假玄武玻璃基质主要由更加细粒的矿物碎屑组成，这些极细粒的矿物碎屑呈棱角状—次圆状(图 3f—g)。但在其形成过程中没有发生熔融或生成的熔体量可以忽略不计(Wenk, 1978; Ozawa and Takizawa, 2007; Pec et al.,

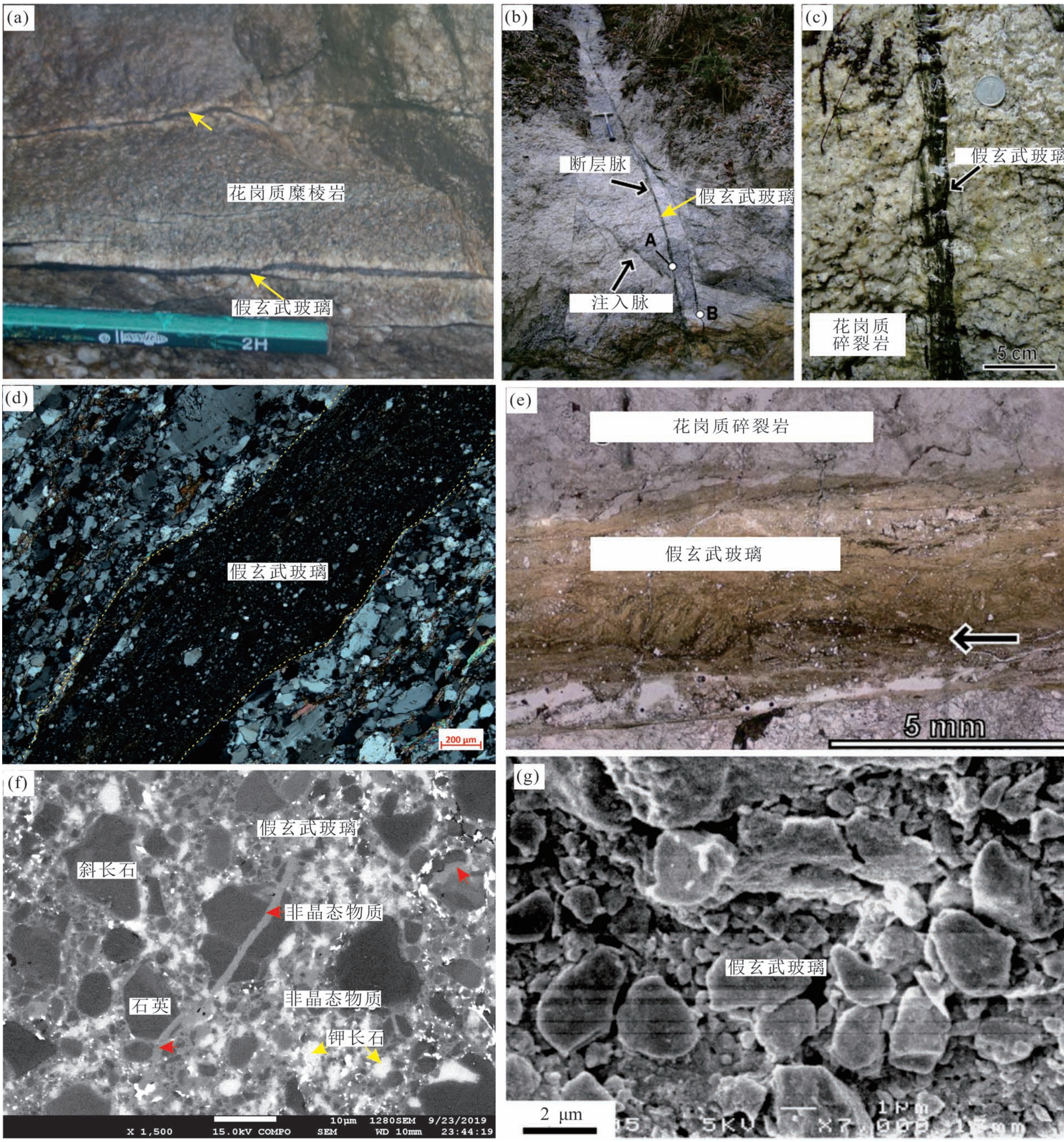

图 3 碎裂成因假玄武玻璃宏观—微观特征

Fig. 3 Macroscopic and microscopic characteristics of pseudotachylyte of cataclastic origin

(a)—(c)呈黑色脉状的假玄武玻璃野外露头照片;(d)细脉状假玄武玻璃及其围岩花岗质糜棱岩显微照片,假玄武玻璃由基质和矿物碎屑两部分组成;(e)假玄武玻璃显微照片,脉体呈黄褐色,发育有流动结构的深褐色薄层(黑色箭头);(f)假玄武玻璃 BSE 显微照片,碎屑主要由棱角状—次棱角状石英、钾长石组成,基质由极细粒的矿物颗粒组成(<1 um),在基质中可见非晶态(脉)材料;(g)假玄武玻璃 HRSEM 照片,可见棱角状—次棱角状的碎屑以及极细粒的基质;照片(a)、(d)、(f)样品采自滇西点苍山南部西洱河断裂附近;照片(b)、(c)、(e)、(g)引自 Ozawa and Takizawa (2007)

(a)—(c) Field outcrops of pseudotachylyte in black veins. (d) Micrographs of veinlet pseudotachylyte and its surrounding granitic mylonite. Pseudotachylyte is composed of matrix and mineral clasts. (e) The pseudotachylyte vein is yellowish brown, and a dark brown thin layer with flowing structure (black arrow) is developed. (f) BSE image of pseudotachylyte. The clasts are mainly composed of angular or subangular quartz and K-feldspar. The matrix is composed of very fine mineral particles (< 1 μm). Amorphous (vein) materials can be seen in the matrix. (g) In the HRSEM photos of pseudotachylyte, angular subangular fragment and very fine-grained matrix can be seen. Samples (a), (d) and (f) in photos were collected near the Xi'er River fault in the south of Diancang Mountains in western Yunnan. Photos (b), (c), (e), (g) is cited from Ozawa and Takizawa (2007)

2012b)。一些研究也报导了自然界中存在的超碎裂成因假玄武玻璃,它们的典型特征是基质主要由极细粒的碎屑组成,只含有少量的非晶态物质,没有典型的熔融结构(Clough, 1888; Wenk, 1978; Wenk and Weiss, 1982; Lin Aiming, 1996; Ozawa and Takizawa, 2007; Janssen et al., 2010; 靳立杰等, 2014)。我们在滇西点苍山发现的碎裂成因假玄武玻璃中也存在有少量的非晶态物质(图 3f)。这种成因机制强调机械粉碎而非摩擦熔融。高压快速摩擦/剪切实验也获得了与宏观下熔融成因假玄武玻璃相似的细脉,但其没有经历熔融,而是高度碎裂化—粉末化的细粒破碎物压实形成的集合体(Weiss and Wenk, 1983; Pec et al., 2012a, 2016)。有学者认为这种假玄武玻璃的成因可归因于地震断裂过程中气—固—液系统中细粒物质的流态化和注入作用(Lin Aiming, 2019)。

判断超碎裂成因假玄武玻璃的明显特征:①假玄武玻璃基质主要由非常细粒且棱角状碎屑组成,几乎没有摩擦熔融的迹象(Lin Aiming, 1996, 1999; Ozawa and Takizawa, 2007)。②假玄武玻璃中碎屑的圆度一般小于 0.4(Lin Aiming, 1999)。③假玄武玻璃的整体化学成分与母岩相似或只有轻微的变化(Lin Aiming, 1996; Ozawa and Takizawa, 2007)。④如果存在非晶态物质,那么这些非晶态物质具有不规则的边界,且表现出介于非晶态与矿物晶体碎片之间的过渡状态(Yund et al., 1990; Ozawa and Takizawa, 2007; Janssen et al., 2010)。根据不同类型假玄武玻璃所具有的显微结构特征,可以较为容易区分超碎裂与摩擦熔融成因假玄武玻璃。然而当摩擦熔融成因的假玄武玻璃经过复杂地质作用改造后(如脱玻化、塑性变形、重结晶作用、流体改造等),原先玻璃质基质发生矿物生长或重结晶形成隐晶或超细粒晶体基质,只从微观结构上很难与超碎裂成因假玄武玻璃区分。在这种情况下,可以通过假玄武玻璃基质与原岩中 SiO_2 的变化规律来加以区分。有学者研究表明,熔融与碎裂成因假玄武玻璃基质/非晶态材料中 SiO_2 含量与原岩变化规律明显不同,熔融成因假玄武玻璃基质中 SiO_2 含量低于原岩(石英熔点高于长石以及镁铁质矿物),而通过地震滑动过程中粉碎作用形成的非晶态物质常伴随着流体—岩石反应和矿物转化,由于 SiO_2 不容易被流体带走,导致形成的非晶态物质 SiO_2 含量通常高于原岩(Dang Jiaxiang and Zhou Yongsheng, 2021)。

2.3　碎裂—熔融相关联成因

除了上述两种对立的观点外,还有另一种认为假玄武玻璃形成与碎裂—熔融都直接关联(Magloughlin, 1992; Kirkpatrick and Rowe, 2013),即粉碎和摩擦诱导熔融是相关过程(Swanson, 1992; Ray, 1999; Fabbri et al., 2000; 林爱明等, 2002; Di Toro and Pennacchioni, 2005; 刘建民等, 2005; 侯广顺等, 2013; 王历星等, 2019)。Spray(1995)通过高速摩擦滑移实验证明,摩擦滑动期间的晶粒尺寸减小是同震滑动期间摩擦熔融的必要前兆(Tsutsumi and Shimamoto, 1997; Hirose and Shimamoto, 2003)。Ray(1999)通过研究假玄武玻璃中的碎屑粒度分布,提出粉碎可能是完整岩石向假玄武玻璃转化的过程之一。岩石的细粒化与摩擦熔融是相辅相成的,而不是相互排斥的过程,粉碎或熔化的发生取决于滑动界面的能量,根本上是取决于应变速率(Spray, 1995)。岩石和矿物的力学性质(这些性质包括屈服强度、剪切屈服强度、断裂韧性和导热系数)控制着粉碎过程(Spray, 2010)。然而,很少有研究能直接证明自然界中假玄武玻璃的粉碎和熔化之间的关系,也很难定义详细的微观结构特征,以建立起两者之间的联系。

2.4　假玄武玻璃形成过程:非稳态流变和地震作用

地震过程往往伴随着断层不稳定滑动,产生强烈的应变局部化带。实验表明,在一定温压条件下当岩石处于半脆性域时可发生非稳态流变,在发生碎裂作用的同时也可发生动态重结晶以及位错蠕变等塑性变形(牛露等,2021)。有学者发现同时存在摩擦熔体和重结晶细颗粒是大多数含假玄武玻璃断裂岩的系统性特征,并通过对重结晶细粒石英和假玄武玻璃显微结构及变形组构的详细研究,揭示了脆—韧性转换带中假玄武玻璃形成是非稳态流变过程(Bestmann et al., 2011, 2012)。在脆—韧性转换带中,形成假玄武玻璃将经历以下 4 个阶段(Bestmann et al., 2012),并且在此过程中石英经历了碎裂—动态重结晶—静态重结晶(图 4a):①同震破裂与碎裂岩形成,在滑动初期断层摩擦较大,地震破裂传播过程中在断层带附近产生大量同震破裂,断层表面延伸出多组高角度裂缝,石英发生初始破碎,形成碎裂岩。同震滑动过程导致温度上升,使得母岩中石英颗粒发育高位错密度。②高应力位错滑移,断层面摩擦剪切加热引起持续升温发生熔融,形成的熔体沿断层面分布并注入到围岩裂隙中。温度的升高促进了位错的发展与重新排列,石英发生动

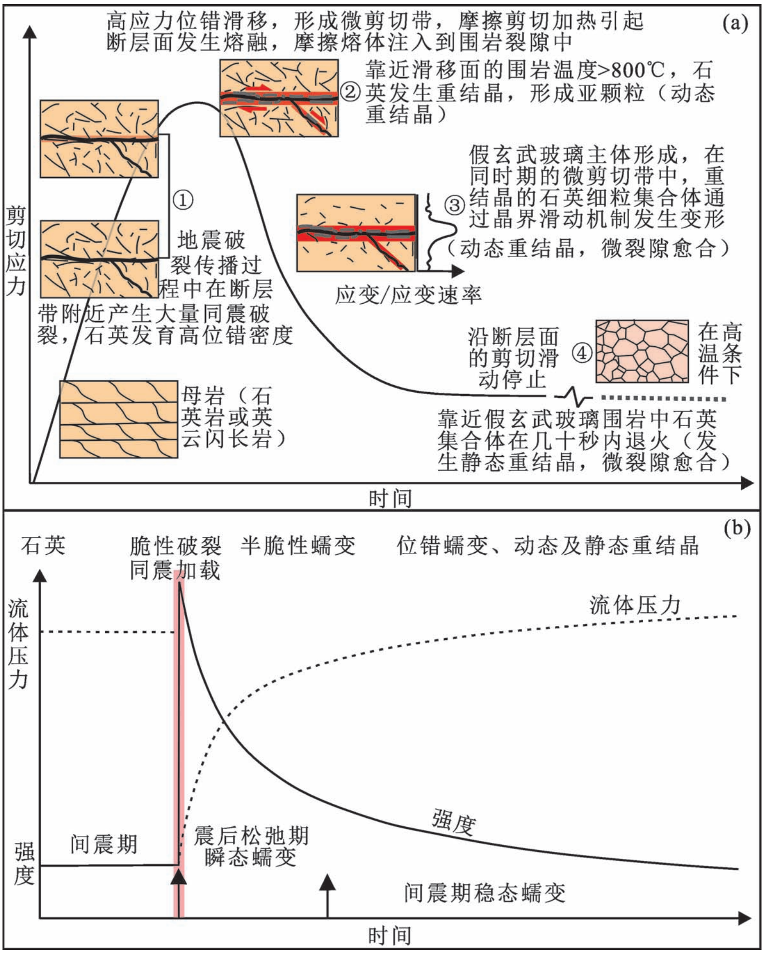

图 4 沿地震断层滑动过程中，断层剪切强度随时间演化的理想化模型及石英显微结构特征(a)(据 Bestmann et al., 2012 修改)和地震不同阶段地震层应力状态、石英变形机制随时间变化模式图(b)(据周永胜和戴文浩,2021 修改)

Fig. 4 Idealized model of time evolution of fault shear strength and microstructure characteristics of quartz during sliding along seismic fault (a) (modified after Bestmann et al., 2012) and the model of stress state and quartz deformation mechanism of seismogenic zones change with time in different stages of earthquake (b) (modified after Zhou Yongzhang and Dai Wenhao, 2021&)

态重结晶,形成亚颗粒(高应力和高应变率共同控制了亚晶粒和新晶粒的粒度)。③整个剪切滑移持续几十秒,假玄武玻璃主体形成。与断层滑动同时代的微剪切带中重结晶的细粒石英集合体通过晶界滑动机制发生动态重结晶,导致持续晶体塑性变形和应变累积,围岩裂隙开始发生愈合。④沿断层面的剪切滑动停止,靠近摩擦熔体层的围岩微剪切区可保持数十秒的高温(T>800℃),石英发生静态重结晶,形成三联点结构,并限制晶粒生长,以最大限度地降低石英集合体的表面能,大部分围岩裂隙得到愈合。

对震后松弛和非稳态流变研究表明,应变速率和流体控制着地震周期不同阶段孕震带的变形机制(图 4b)(戴文浩和周永胜,2019;周永胜和戴文浩,2021)。在间震期,孕震带应力以及应变速率较低,在较高的流体压力背景下往往发生稳态蠕变,此时孕震带中长石的主要变形机制以碎裂为主,石英、云母等矿物的变形机制主要以塑性变形为主(如动态重结晶)。在同震破裂阶段,孕震带所受应力较大,应变速率达到最高,断层脆—韧性转换深度增加,伴随强烈的地震破裂,且在较短的持续时间内,发生高速摩擦滑动并伴随有较大的应力降与流体压力降,此阶段断层带中岩石变形机制多以碎裂作用为主,在断层面附近可能形成有假玄武玻璃。而在震后松弛阶段,所受应力逐渐降低,在该阶段断层脆—韧性转换深度变浅,孕震带发生半脆性非稳态流变,其中石英的变形机制以动态和静态重结晶为主,在重结晶作用下地震裂隙开始被愈合,流体压力也逐渐恢复(周永胜等,2014;戴文浩和周永胜,2019;牛露等,2021;周永胜和戴文浩,2021)。

研究表明非稳态流变的物理机制为矿物晶体内位错过程显著大于恢复过程,位错缠结导致晶体强度随应变增加,在持续高应力状态下,微裂隙叠加于晶体塑性变形之上(周永胜和戴文浩,2021)。有学者认为,除了同震破裂过程中形成的假玄武玻璃外,非稳态流变过程中形成的碎裂岩(以及相互叠印愈合的微裂隙和重结晶颗粒)也可作为同震破裂及震后松弛变形的岩石记录(Song Wonjoon et al., 2020;周永胜和戴文浩,2021)。戴文浩和周永胜(2019)对红河断裂带糜棱岩中发育的碎裂岩研究表明,在震后松弛阶段孕震带的变形特征主要以脆性破裂、裂隙愈合以及裂隙中愈合矿物(如石英、方解石等)发生新的塑性变形为主。实验研究表明,在震后松弛非稳态流变状态下,断层裂隙愈合程度对断层强度有着显著的积极影响,随着愈合程度的增加,断层强度逐渐增加,甚至可以恢复到完整岩石的强度(周永胜和何昌荣,2009;牛露等,2018;周永胜和戴文浩,

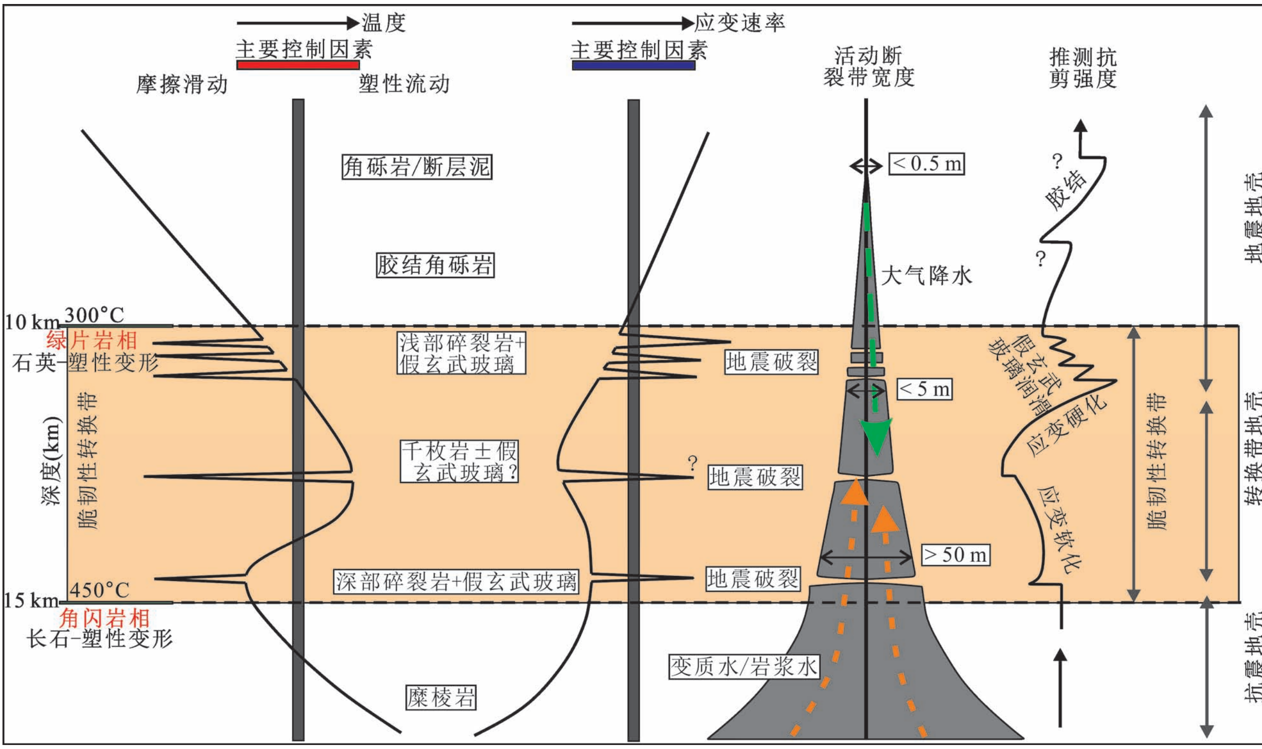

图 5 脆—韧性转换带岩石抗剪强度及控制因素示意图。深度值是以全球大陆平均地温梯度 30℃/km 换算（据 Sibson，1977 修改）

Fig. 5 Schematic diagram of rock shear strength and control factors in brittle ductile transition zone. The depth value is converted by the global continental average geothermal gradient of 30℃ / km (modified after Sibson, 1977)

2021)。

3　假玄武玻璃形成深度与地震成因

地震的发震深度受断层带强度以及滑动摩擦的稳定性控制(周永胜等,2014),在地质时间尺度上,地震破坏经常发生在冷的脆性上地壳。与地震破裂相关的高差应力出现在大陆地壳岩石圈强度最大的区域,即脆—韧性转换带(周永胜和何昌荣,2009;张媛媛和周永胜,2012;刘俊来,2017)。脆韧性转换带一般位于地壳深度 10~15 km 之间,温度约为 300~450℃,刚好处于石英可以发生塑性变形而长石仍以脆性破裂为主的半脆性变形域中,温度和压力显著控制着脆—韧性转换过程及岩石强度(图 5)。脆—韧性转换带中岩石处于流变不稳定状态,在温度、压力、流体作用控制下,易发生应变弱化,从而在地壳中形成弱化带,导致地震、滑坡等地质灾害的发生。与之对应的现象是,目前世界上所报导的假玄武玻璃大多形成于脆—韧转换带及其之上脆性地壳(<15 km,图 5,图 6a)。

地壳浅部(<6 km)富水条件下形成的假玄武玻璃通常发育有气泡和杏仁体结构,而很难观察到韧性变形条件下形成的位错蠕变或扩散蠕变现象。有学者根据这些结构提出两种估算其形成深度的方法:①根据气泡形成时熔体的水含量与静岩压力之间的关系,反推形成深度(Toyoshima, 1990; Lin Aiming, 1991, 1994a);②通过保存在假玄武玻璃中气泡和杏仁体所占的体积百分比来估算静岩压力,通过静岩压力反推形成深度(Maddock et al., 1987; Lin Aiming, 1991, 1994a)。

脆—韧性转换带之下的韧性区域中假玄武玻璃报导较少,原因可能有:①传统上认为在脆—韧性转换带以下(~15 km)变形通常是由晶体塑性变形机制调节的,而地震是一种快速的脆性破裂活动,深部地震不应该发生或频率相对浅源地震频率低;以及②地球深部产生的假玄武玻璃在形成后以及在剥露过程中更加容易被随后的变质变形所改造。但深部地震的却存在,近年来随着研究的深入,脆韧性转换带之下由断层面摩擦熔融形成的假玄武玻璃的报导也逐渐增多(如 Moecher and Steltenpohl, 2011, 约 22~40 km; Clerc et al., 2018, 约 30~50 km;

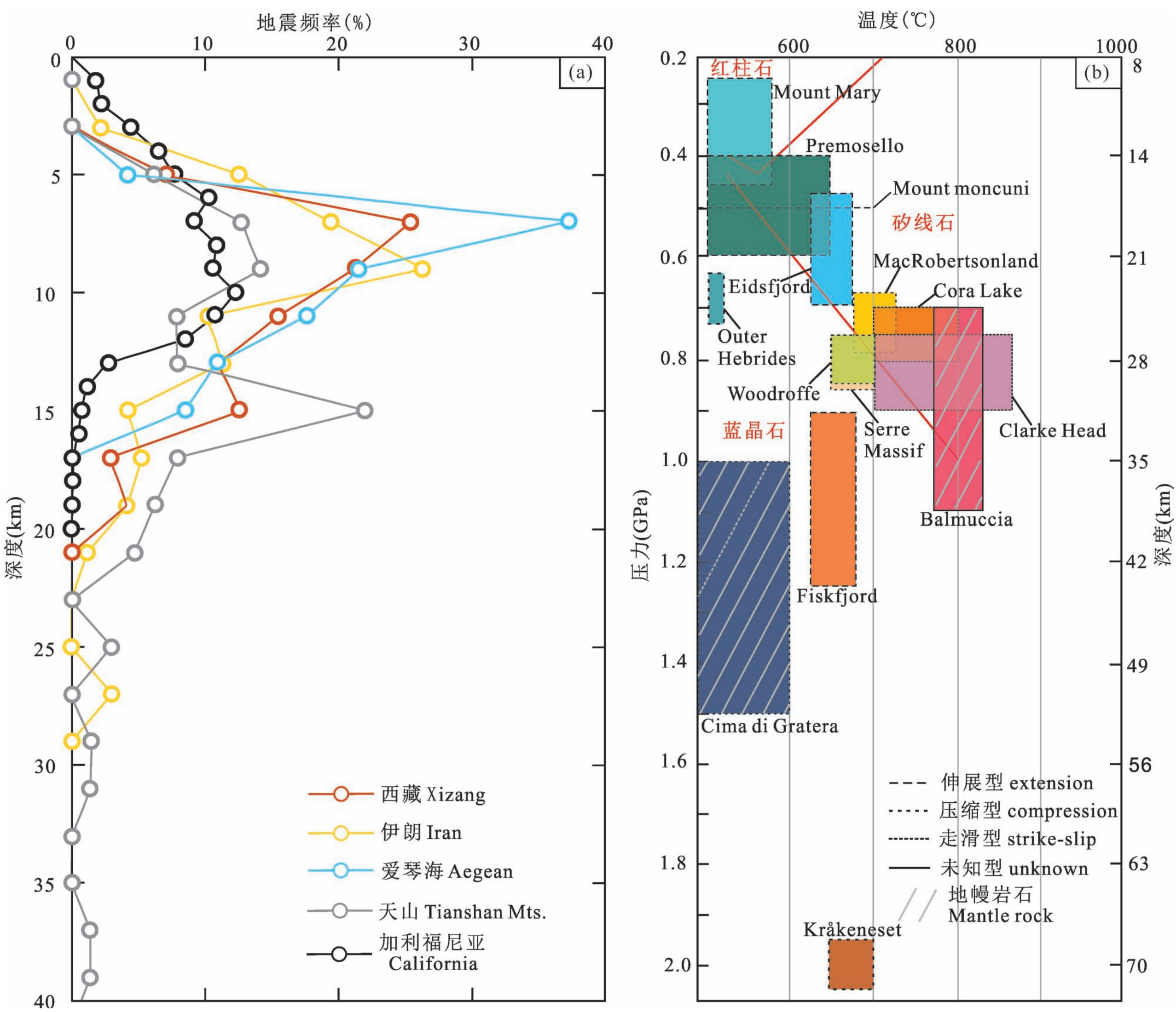

图 6 大陆孕震层和假玄武玻璃的形成深度

Fig. 6 distribution of seismicity frequency and depth of continental seismogenic layer and formation depth of pseudotachylyte

(a)大陆孕震层地震活动频率和深度分布(Passelègue et al., 2021)。(b)形成于地球深部脆—韧性转换带之下假玄武玻璃的压力—温度(P—T)范围图(Orlandini et al., 2019)。右轴的深度值是以 Cora Lake 剪切带温压条件并以 25℃/km 的地温梯度换算的

(a) Distribution of seismicity frequency and depth of continental seismogenic layer (Passelègue et al., 2021). (b) Pressure temperature (*P—T*) range diagram of pseudotachylyte formed under the brittle— ductile transition zone in the deep Earth (Orlandini et al., 2019). The depth value of the right axis is converted based on the temperature and pressure conditions of the Cora Lake shear zone and the geothermal gradient of 25 ℃ / km

Orlandini et al., 2019, 约 24~28 km),甚至有学者报导了上地幔深度所形成的假玄武玻璃(如 Austrheim and Boundy 1994; >60 km; Lund and Austrheim, 2003, >60 km; Scambelluri et al., 2017, 60~70 km; Ferrand et al., 2018, 约 42±8 km)。如图 6b 所示,在 0.4~1.2 GPa(甚至 2 GPa),550~800℃条件下,仍有假玄武玻璃的分布(Orlandini et al., 2019)。这些假玄武玻璃的存在表明在高机械强度和典型孕震区之下也存在大量的地震行为,表明在古地震发震带内不同深度都可能发生快速灾难性位移(Clarke and Norman, 1993; White, 1996; Andersen et al., 2008; Rowe and Griffith, 2015; Moecher and Steltenpohl, 2011; Ferrand et al., 2017; Hawemann et al., 2019)。近些年的研究表明脆—韧性转换带之下的地球深部韧性域的局部弱化是导致脆性破裂产生从而形成假玄武玻璃的重要原因,但对深部高压条件下地震传播所需的同震弱化机制还存在很大争议(本文 7.2 节),这要求我们需要重新认识脆—韧性转换带之下岩石的变形机制。

总结来说,断层相关的假玄武玻璃可以在不同

的深度产生,从靠近地表的浅部地壳到下地壳的深部剪切带,甚至是在浅部地幔内(60~70 km)。在脆—韧性转换带之下区域发现的假玄武玻璃为中、深尺度存在地震提供了有力证据(图 6b),但地震如何发生在脆—韧性转换带之下的下地壳和上地幔深度至今仍是一个争议的关键问题。

4　流体在假玄武玻璃形成过程中的作用

流体广泛存在于地球的各个圈层,对岩石流变强度及变形机制有着显著的影响(刘贵和周永胜,2012)。流体(水)在促发地震中的作用已经争论了很久(Scholz et al., 1973; Sibson, 1994)。已有大量证据表明,流体和孔隙压力的演化可以影响地震破裂、影响地震的成核过程(Sibson, 1986; Collettini et al., 2005; 周永胜和何昌荣,2009)。有学者认为流体诱导引发的脆性破坏是深部地震的一个重要成因(Kirby et al., 1996; Hacker et al., 2003; Ferrand et al., 2017)。作为地震滑移的产物,通过研究流体在假玄武玻璃形成过程中扮演的角色,可以为地震的成因机制提供宝贵的见解。

虽然学者们进行了大量理论与实践的研究,但关于流体在假玄武玻璃形成过程中的作用还存在很多争议。早期一般认为干燥的断层带有利于假玄武玻璃的形成,因为水(流体)的存在会降低断层表面的有效正应力,从而降低给定摩擦系数(μ)的剪切强度(τ),不利于热量的积累以及摩擦熔融的进行(Sibson, 1973; Bizzarri and Cocco, 2006a, b; Rice, 2006; Viesca and Garagash, 2015; Proctor and Lockner, 2016; Acosta et al., 2018)。

地震滑移产生热量 q 可以由公式计算:

$$q=\tau x \quad (1)$$

其中 τ 是断层的平均剪切应力,x 是断层的位移。而断层的平均剪切应力可以由公式计算:

$$\tau=\mu(\sigma_n-P_f) \quad (2)$$

其中 μ 是动态摩擦系数,σ_n 是垂直于断层面的正应力,P_f 是流体孔隙压力,在流体存在的情况下,岩石的剪切阻力(τ_f)一般小于干燥断裂带的剪切强度 τ。由公式(1)、(2)组合可以得出:

$$q=\mu(\sigma_n-P_f)x \quad (3)$$

由公式(3)我们可以发现地震滑移产生的热量 q 与流体孔隙压力有关,当流体孔隙压力接近法向应力时,断层面产生的热量趋于零(O´Hara and Sharp, 2001)。其次,流体也可能导致石英或其他硅酸盐矿物发生水解弱化(Griggs, 1967; Freiman, 1984),导致 Si—O 共价键被 H—O 键代替从而促进岩石塑性变形。Proctor 和 Lockner(2016)利用干样品(干花岗岩)和湿样品(湿花岗岩)进行的摩擦滑移实验结果表明,湿花岗岩的熔融温度虽然比干花岗岩低,但滑移表面产生的摩擦熔体较少。虽然滑移面上少量的水可以吸收几焦耳的热量,但这些热量与滑移面摩擦产生的热量相比很少,不足以抑制摩擦熔融,因此他们认为可能是由孔隙水在滑移事件期间通过热增压,促进滑动表面的膨胀,并抑制摩擦加热和熔化"焊接",同时水的热增压作用可以使湿样品在较低的剪切作用下发生黏滑事件。

但也有学者认为流体(水)的存在下有利于断层面的摩擦熔融,从而形成假玄武玻璃。因为流体的存在可以降低单矿物的熔融温度,以及形成较低黏度的熔体(Ermanovics et al., 1972; Allen, 1979; Maddock, 1992; Lin Aiming, 1994a)。而且 Brantut 和 Mitchell(2018)已经证明,如果断层面的流体可以及时发生迁移,孔隙流体的热增压机制可以被抑制,从而导致破裂面上发生快速摩擦熔融。事实上天然存在的假玄武玻璃可能是在湿断层中产生的,不一定需要干的环境(Magloughlin, 1992; Rowe et al., 2005; Griffith et al., 2010; Deseta et al., 2014b)。理论和实验证明选择性熔融优先发生在富水矿物中,如云母、角闪石等(Allen, 1979; Lin Aiming, 1994a; Maddock, 1992; Spray, 1992, 2010)。Dixon 和 Dixon(1989)通过计算表明,假玄武玻璃基质中气泡的存在是由于在摩擦熔体冷却过程中夹带有挥发份,因为冷却过程没有足够的时间通过脱气形成气泡(Maddock et al., 1987)。此外摩擦熔融实验结果也表明,摩擦熔体可以在富含水的环境中产生(Killick, 1990; Kennedy and Spray, 1992),或者含水矿物的脱水反应可以触发断层带的剪切破坏,有助于断层面的摩擦熔融(Green, 1995; Jung Haemyeong et al., 2004, 2006; Ferrand et al., 2017)。丰富的含水矿物在高应变率变形过程中发挥了强大的流变控制作用,促进了热触发剪切不稳定性(Brantut et al., 2011; Deseta et al., 2014b; Yamashita and Schubnel, 2016)。很多天然产出的假玄武玻璃的含水量一般比母岩高(Toyoshima, 1990; Lin Aiming, 1991, 1994a),假玄武玻璃或其围岩中含有不同量的含水矿物,如透闪石、角闪石、蓝闪石、蛇纹石、绿泥石、绿帘石(Griffith et al., 2010; Deseta et al., 2014b; Magott et al.,

2020)，但值得说明的是目前仍很难确定假玄武玻璃形成时就含水量高还是形成后由于水岩反应吸收了水导致断层带中富集这些含水矿物。因为大位移走滑断裂的同震产生的损伤区(断层动态滑动面周围高度破碎的岩石)可以延伸到孕震带底部，影响断层及周围岩石渗透率，控制流体流动和流变变化(Song Wonjoon et al.，2020)。同震破碎带的存在很容易使断层带岩石受外界流体干预，发生流体交代事件，甚至同震变形后的震后松弛阶段的重结晶作用也可改变岩石流体包裹体丰度，从而影响水含量(Song Wonjoon et al.，2020)。

流体(水)的来源也是学者们比较关心的科学问题之一，通常需要考虑两种不同类型的水，即它们是来自于含水矿物的脱水(Allen，1979；O'Hara，1992)，或者从外界进入断层带的孔隙水(Lin Aiming，1994a)。O'Hara 和 Sharp(2001)提出可以通过氧同位素组成变化来判断假玄武玻璃形成过程中水的来源，含水矿物的脱水将在较高的温度(如1000℃)下进行且会与假玄武玻璃相互作用，从而使熔体和水之间的同位素分馏很小，而孔隙水具有较低的 $\delta^{18}O$ 值，能够降低熔体的同位素值。但通过氧同位素判断是从外界进入到断层中的水时，要从宏观和微观及其他证据确定这些外来水是假玄武玻璃形成前就存在，还是假玄武玻璃形成后通过风化蚀变、水化作用进入到假玄武玻璃中。

流体(水)的存在对断层面摩擦熔体的产生既有不利因素(降低断层表面的有效正应力、降低剪切强度 τ、促进晶体塑性变形)，也有有利因素(降低单矿物的熔融温度、形成较低黏度的熔体、有利于断层面滑移的启动)，流体在假玄武玻璃形成过程中扮演什么样的角色需要我们综合考虑断层带所处的温压、应力状态，以及断层岩的物理性质，如热容量、热扩散率、孔隙储存容量、水扩散系数、孔隙空间的热膨胀性，以及滑动诱导的膨胀/压实系数。

在地震破裂过程中必然存在某种弱化机制，在断层滑动累积时迅速降低断层的强度，否则在狭窄的断层带中温度将迅速升高，显著超过大多数岩石的固相线温度而发生大规模的熔融。这与地质事实不符，因为断裂带中形成的假玄武玻璃的体积通常都很小。流体(水)存在所形成的热增压效应，是一种普遍接受的弱化机制(Rice，2006；Viesca and Garagash，2015；Brantut，2020)，并且流体可将岩石的熔融温度降低到远低于岩石的固相线温度，从而确保熔融只在断层面附近发生。当处于干断层面环境时，断层面不存在引起显著热增压效应的流体，摩擦加热所累积的温度达到断层面岩石的熔融温度后，断层面岩石发生选择性熔融，当产生的熔体量达到一定程度时，也会引起断层的弱化作用(Hirose and Shimamoto，2005)，使断层带的岩石不能发生大规模的熔融。

5 假玄武玻璃形成后对断层强度的影响

当构造荷载引起的应力达到断层破裂强度时，随后就将发生地震。地震断层发生剪切滑动过程中，当围岩的热扩散性较低时，热量的积累会使断层面温度迅速升高，当温度达到断层面矿物的最低熔点时就会发生选择性熔融，熔融产生的熔体夹带着一定量的断层碎屑快速冷却形成假玄武玻璃(Sibson，1975；Spray，1992)。实验研究表明摩擦熔融产生的熔体可以对断层带力学强度产生重要影响(Hirose and Shimamoto，2005；Di Toro et al.，2006；Niemeijer et al.，2011；Kendrick et al.，2014；Hornby et al.，2015)。在断层滑动过程中摩擦熔体既可以充当润滑剂，大幅降低滑动期间的摩擦阻力(McKenzie and Brune，1972；Tsutsumi and Shimamoto，1997；Hirose and Shimamoto，2005；Di Toro et al.，2006；Hung Chiencheng et al.，2019)，也可以充当黏性抑制剂，导致滑动速度减弱和地震滑动的终止(Koizumi et al.，2004；Kendrick et al.，2014；Proctor and Lockner，2016；Mitchell et al.，2016；Hayward and Cox，2017)。关于地震滑动时断层润滑效应还有非常多的模型来解释，如闪热(Rice，2006；Beeler et al.，2008；Goldsby and Tullis，2011)、粉末润滑(Han et al.，2010；Reches and Lockner，2010)、硅胶润滑(Di Toro et al.，2004)、热分解(Han et al.，2007；Collettini et al.，2013)、弹性流体动力润滑(Brodsky and Kanamori，2001；Cornelio et al.，2019)等方式。

断层面上熔体的润滑与抑制作用是动态变化的。当熔体形成后会导致断层面摩擦强度显著降低，熔体起到显著的润滑作用。但当断层因熔体的润滑作用而被削弱后，摩擦阻力不足以产生足够的热量来进一步驱动熔体产生时，熔融体会迅速冷却并凝固形成假玄武玻璃，固结的假玄武玻璃可能会导致断层强度的恢复，从而起到黏性抑制作用(Proctor and Lockner，2016)。为了详细解释摩擦熔体对断层失稳的影响过程，学者们做了大量的摩擦

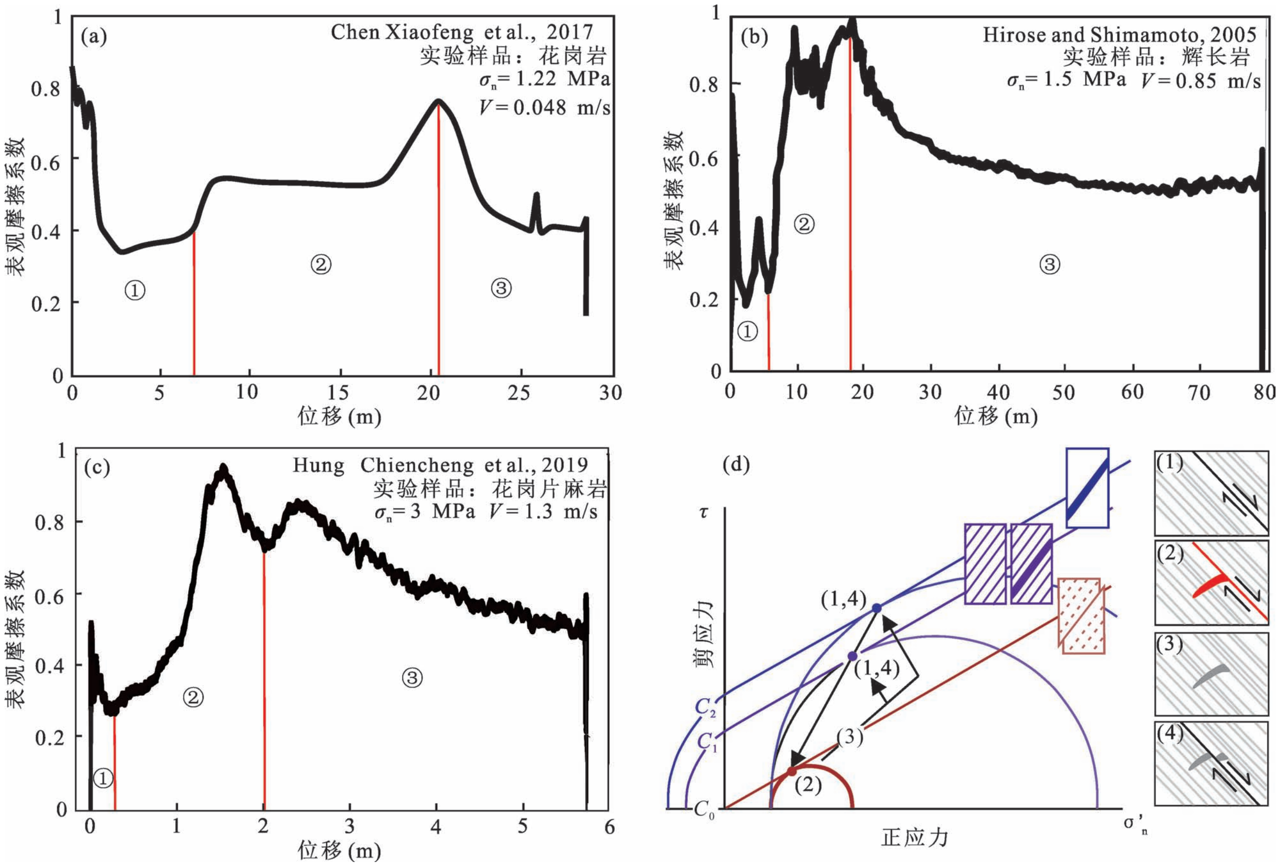

图 7 结晶硅酸盐断层面表观摩擦系数随位移演化示意图

Fig. 7 Evolution of apparent friction coefficient of crystalline silicate fault surface with displacement

(a)花岗岩在 1.22 MPa 法向正应力以及 0.048 m/s 剪切滑移速度下,表观摩擦系数随位移演化示意图(参考 Chen Xiaofeng et al., 2017);(b)辉长岩在 1.5 MPa 法向正应力以及 0.85 m/s 剪切滑移速度下,表观摩擦系数随位移演化示意图(参考 Hirose and Shimamoto, 2005);(c)花岗片麻岩在 3 MPa 法向正应力以及 1.3 m/s 剪切滑移速度下,表观摩擦系数随位移演化示意图(参考 Hung Chiencheng et al., 2019);(d)含假玄武玻璃岩石破坏模式演化示意图(参考 Mitchell et al., 2016)。强度关系用带有线性库仑包络线的摩尔圆示意图表示;C_1 和 C_2 分别代表 Alpine 断裂(新西兰)糜棱岩和 Gole Larghe 断裂(意大利)英云闪长岩的粘结强度,C_0 代表两种岩石在断裂和无黏性时的粘结强度;τ 为剪应力,σ_n 为正应力

(a) Evolution of apparent friction coefficient with displacement of granite under 1.22 MPa normal stress and 0.048 m/s shear slip velocity (Chen Xiaofeng et al., 2017); (b) apparent friction coefficient with displacement of gabbro under 1.5 MPa normal stress and 0.85 m/s shear slip velocity (Hirose and Shimamoto, 2005); (c) friction coefficient with displacement of granite gneiss under 3 MPa normal stress and 1.3 m/s shear slip velocity (Hung Chiencheng et al., 2019); (d) failure mode evolution of pseudotachylyte containing rocks (Mitchell et al., 2016). The strength relationship is represented schematically by a molar circle with a linear Coulomb envelope. C_1 and C_2 represent the cohesive strength of mylonite in Alpine fault (New Zealand) and tonalite in Gole Larghe fault (Italy), respectively, and C_0 represents both rocks when faulted and cohesionless. τ is the shear stress, σ_n is normal stress

熔融实验。不同实验条件下以及不同的实验样品会产生不同的实验结果,但大多数实验表明,断层面岩石的摩擦强度演化都存在 3 个阶段,初始弱化—强化—二次弱化(Hirose and Shimamoto, 2005; Chen Xiaofeng et al., 2017),或初始弱化—先加强后略微弱化—第二次加强后最终衰减向稳态值(Hung Chiencheng et al., 2019)。Chen Xiaofeng 等(2017)认为最初的弱化是断层带表面粉末润滑引起的,然后强化阶段是由于初始熔体的体积膨胀以及黏性抑制作用,最后的弱化阶段是熔体量达到临界点后引起的熔体润滑(图 7a)。而 Hirose 和 Shimamoto(2005)认为最初的弱化与闪热作用有关,第二次弱化与熔体形成熔融层导致的熔体润滑有关(图 7b)。最近研究认为,初始阶段的弱化是由于断层面岩石表面的颗粒破碎和闪热弱化所致、第二阶段的断层强化是由于高黏度(温度较低,黏度较大)摩擦熔体的形成所致,第三阶段初始断层再强化与熔体黏度增加有关,主要是由于摩擦熔体的 SiO_2 富集所致,

最终的弱化是由于覆盖整个滑动面的连续熔融层的形成以及熔体温度升高而降低了黏度,形成熔体润滑效应(图 7c)(Hung Chiencheng et al., 2019)。

Mitchell 等(2016)利用含假玄武玻璃的天然岩石(糜棱岩)进行摩擦熔融实验,他们认为地震滑移过程中断层粘结强度的演化包括 4 个阶段(图 7d),① 在岩石薄弱面上发生初始破坏;② 断层稳定滑动,在黏滑条件下产生摩擦熔体并导致断层弱化;③随着摩擦熔体的冷凝,断层强度逐渐恢复;④ 在随后的剪切滑动作用下,(亚)平行于先前断层面的新断层滑动面上发生破坏。他们的实验结果表明在冷且干燥以及相对较低的围岩应力(即上地壳条件)条件下,假玄武玻璃会在同震滑动停止后迅速"焊接"断层面,加强断层强度。所以假玄武玻璃的形成是一种重要的动态弱化机制,但不是一种地壳断裂带中长期的弱化机制,因为凝固后的假玄武玻璃会使断层强度恢复到未产生摩擦熔体的强度(Proctor and Lockner, 2016; Mitchell et al., 2016)。

6 假玄武玻璃的保存与改造

假玄武玻璃作为地震事件的"化石"记录已被学者广泛接受,但与活动断层中地震的频率和分布相比,断层带中天然假玄武玻璃的报导是非常罕见的(Kirkpatrick and Rowe, 2013)。尤其是超基性岩石中报导的假玄武玻璃非常少,在全世界范围内目前只在这些地区曾报导过:Corsica(Andersen and Austrheim, 2006, Deseta et al., 2014a; Maggot et al., 2016)、Balmuccia, Italy(Obata and Karato, 1995; Ueda et al., 2008; Ferrand et al., 2018; Ueda et al., 2020)、Lanzo, Italy(Piccardo et al., 2010; Scambelluri et al., 2017)、Horoman, Japan(Morishita, 1998)、Cerro del Almirez massif, Spain(Evans and Cowan, 2012)。我们认为假玄武玻璃报导较少的原因主要有:① 地震过程中断层摩擦熔融被抑制。在上节中我们简单提到了地震断层滑动时存在很多润滑机制,以及熔体形成后也会产生熔体润滑效应,这些润滑效应导致断层面很难生成熔体或生成熔体的量有限;② 在活跃断层带中假玄武玻璃形成后,由于后期地质事件的改造、风化剥蚀等原因难以保存下来(Sibson and Toy, 2006; Kirkpatrick et al., 2009; Kirkpatrick and Rowe, 2013)。

假玄武玻璃形成后很难保存也是目前假玄武玻璃较少地被发现或报道的重要原因之一。由于假玄武玻璃中存在亚稳态的玻璃或极细粒的基质,导致

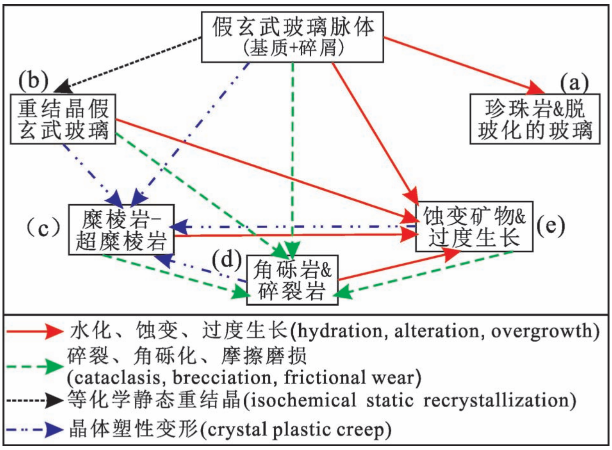

图 8 可能破坏假玄武玻璃的演化路径流程图(据 Kirkpatrick and Rowe, 2013 修改)

Fig. 8 Flow chart for evolution path which may destroy the rock record of pseudotachylyte (modified after Kirkpatrick and Rowe, 2013)

(a)简单的水化作用可能会使假玄武玻璃形成脱玻璃化的物质,它仍然可以被鉴定为以前的玻璃状物质;(b)等化学静态重结晶可能破坏假玄武玻璃脉体的微观结构,但同时可以保留宏观脉体的几何形状;(c)晶体塑性变形可能使假玄武玻璃初始显微结构发生粗化和重结晶,以及使初始脉体的几何形状发生变形;(d)碎裂作用可以破坏假玄武玻璃脉体的宏观结构,但仍可观察到假玄武玻璃的显微结构特征;(e)蚀变和过度生长可能会保留假玄武玻璃脉体的整体几何结构,但会使原生显微结构逐渐模糊以至于完全消失

(a) Simple hydration may cause pseudotachylyte to form devitrified material, which can still be identified as previous glassy material; (b) isochemical static recrystallization may destroy the microstructure of pseudotachylyte veins, but it can retain the geometry of macro veins at the same time; (c) crystal plastic deformation may coarsen and recrystallize the initial microstructure of pseudotachylyte, and deform the geometry of the initial vein; (d) fragmentation can destroy the macro structure of pseudotachylyte veins, but the microstructure characteristics of pseudotachylyte can still be observed; (e) alteration and overgrowth may preserve the overall geometry of pseudotachylyte veins, but will gradually blur the primary microstructure and disappear completely

假玄武玻璃相比于围岩更容易遭受后期改造(Kirkpatrick and Rowe, 2013)。以下过程将导致假玄武玻璃的一些主要特征发生改变,变得不易识别(图 8):①等化学静态重结晶:由于假玄武玻璃含有玻璃质或隐晶质(非常细粒,处于亚稳态)基质,使得假玄武玻璃特别容易发生重结晶,用不同的晶体结构取代初始矿物或玻璃结构,同时保持全岩化学组成不变。在流体(水)存在下,先前形成的假玄武玻璃或微晶体结构很容易发生重结晶。②水化蚀变:水化不同于等化学重结晶,固相和流体相之间的

阳离子交换会引起蚀变。常见的水化矿物有绿泥石、绿帘石、伊利石、蒙脱石。新形成的矿物可能部分或者完全覆盖原始的微观结构。有学者研究表明玄武质玻璃的水化是通过同成分的二氧化硅溶解实现的,硅被添加到流体中,在玻璃表面留下硅耗尽的硅酸盐沉淀物(Crovisier et al., 1987; Morin et al., 2015)。③碎裂改造:将假玄武玻璃碎裂成更小的碎片,形成碎裂岩,使原始的结构被破坏,碎裂作用可导致假玄武玻璃的碎片分布在不同的断层岩石组合中。④塑性变形叠加:塑性应变局部化会导致假玄武玻璃基质出现晶体生长、重结晶、晶体优选定向,假玄武玻璃中残留的碎屑也可能受到改造,发生塑性变形(旋转拉长,形成拖尾)。也许在脆—韧性转换带(存在广泛的应变速率)中,碎裂岩、摩擦熔融体和塑性变形晶体在不同应变速率下反复交叉、叠印出现,而温度、应变速率、压力和流体控制着假玄武玻璃的演化路径。由于假玄武玻璃极容易被后期地质事件改造,如晶体塑性变形、重结晶、水化蚀变、碎裂作用,使其变得较难识别。但进一步的研究表明,有些假玄武玻璃的识别标志可能不会随地质改造以及时间的变化而消失,如假玄武玻璃的冷凝边是由于摩擦熔体与围岩之间极端的温度梯度而形成,越接近围岩粒度越细,脉体边缘可能呈隐晶质或玻璃质,当经历重结晶作用后,原始矿物的粒度会改变,但这种粒度的梯度可能会保留,或当经历碎裂变形后,会保留有隐晶质—微晶质、玻璃质碎片,这些残存的特征可以帮助更好的识别被改造的假玄武玻璃(Kirkpatrick and Rowe, 2013)。

有一个很有意思的现象是世界上报导的假玄武玻璃多产自于结晶程度较好的岩石中,特别是在长英质侵入岩中,而玄武岩中关于假玄武玻璃的报导很少。但玄武岩是俯冲带大逆冲断层的主要组成部分之一,而俯冲带是世界上最大的地震发生地,鲜有假玄武玻璃的发现是值得探讨的问题。有学者研究表明假玄武玻璃的水化作用在俯冲环境中更容易发生,因为在俯冲环境中,沿着俯冲板片的脱水反应和沉积物的压实作用,会产生稳定的流体供应(Hyndman and Peacock, 2003; Ujiie and Kimura, 2014)。最近,Phillips 等(2019)认为玄武质成分的假玄武玻璃更容易发生水化蚀变,在理想条件下用层状硅酸盐交代玄武岩成分的假玄武玻璃所需的最短时间小于 11 h,而交代相同厚度的流纹岩成分的假玄武玻璃则需要 5 年,与大多数地质过程相比,这种改造速率非常快,这有助于我们理解为什么在俯冲带中(特别是俯冲带中的玄武岩中)很少保存有假玄武玻璃(Sibson and Toy, 2006; Phillips et al., 2019)。另一个重要的原因是假玄武玻璃粒度非常细,颜色与玄武岩颜色相近,导致用肉眼很难在玄武岩中识别出假玄武玻璃岩脉,而长英质或其他浅色岩石与深色的假玄武玻璃岩脉颜色对比明显,在野外更容易识别(Sibson and Toy, 2006; Kirkpatrick et al., 2009)。

7　讨论

7.1　碎裂成因假玄武玻璃中非晶态物质形成机制及影响

假玄武玻璃中的非晶态物质通常归因于陨石冲击或摩擦加热导致的熔融(Philpotts, 1964; Sibson, 1975, 1980; Passchier, 1982; Magloughlin, 1992)。然而,升温和热力学熔化并不是从晶态到非晶态转变的唯一方法。非晶态物质可以通过多种方式产生,例如摩擦熔体的快速冷却(Toyoshima, 1990; Lin Aiming, 1994a; Obata and Karato, 1995; Incel et al., 2017),化学反应(Rahier et al., 1996, 1997; Duxson et al., 2007),热液蚀变(Henley and Ellis, 1983),增加压力(Hemley et al., 1988; Tomioka et al., 2010),以及碎裂/粉碎(Yund et al., 1990; Pec et al., 2016)。

地震破裂和摩擦熔融过程中形成的假玄武玻璃是断裂带中最常见的非晶态物质。但关于假玄武玻璃中的非晶态物质是在熔融过程还是碎裂/粉碎过程中形成存在不同的见解。大多数的非晶态物质归因于地震滑动过程中的摩擦熔融(McKenzie and Brune, 1972; Sibson, 1975; Obata and Karato, 1995; Hirose and Shimamoto, 2005; Scambelluri et al., 2017)。但不能仅根据存在非晶态物质而将假玄武玻璃判断为熔融成因或者形成过程中发生了熔融。近些年的研究表明碎裂成因假玄武玻璃中的非晶态物质可以通过碎裂/粉碎过程中机械能引起的机械—化学效应形成(Yund et al., 1990; Ozawa and Takizawa, 2007; Janssen et al., 2010; Pec et al., 2012a, b, 2016; Hayward et al., 2016; Marti et al., 2020; Dang Jiaxiang and Zhou Yongsheng, 2021)。粉碎可以在机械应力(如剪切应力和冲击应力)下诱导固态相变,使得晶体材料逐渐无序化,最终转变为非晶态材料(Hemley et al., 1988; Wolf et al., 1990; Yund et al., 1990; Yip et al., 2005; Di Toro et al., 2004; Pec et al., 2012a, b, 2016;

Rowe et al., 2019; Marti et al., 2020)。而且有实验表明,斜长石特别容易通过机械粉碎进行非晶化(Marti et al., 2020; Pec et al., 2012b)。例如,在高差应力下,斜长石晶体形成非晶态材料只需要几毫米的位移量(Marti et al., 2020)。Ozawa 和 Takizawa(2007)也报道了天然碎裂成因假玄武玻璃中的非晶态材料,它们是由粉碎过程中的机械磨损而不是熔体的快速冷却形成的。我们在滇西点苍山变质杂岩体中发现的碎裂成因假玄武玻璃中也观察到非晶态物质(AM)的存在(图 3f),且而这些非晶态物质与斜长石存在密切关系。

虽然现在大多数地质学家都认同断层成因的假玄武玻璃是古地震引起的断层快速活动发生破裂—熔融的直接产物,其可作为古地震活动的直接证据。但自然界还存在一类非震断层(蠕滑型断层),一般表现为连续缓慢地滑动,不诱发地震活动。变形实验表明在一系列温度、正应力以及位移速率下均可产生非晶态物质(Spray, 1987; Yund et al., 1990; Goldsby and Tullis, 2002; Di Toro et al., 2006; Niemeijer et al., 2011; Pec et al., 2012a, b, 2016; Hayward et al., 2016; Marti et al., 2020)。有学者的实验研究表明,非晶态物质可以在接近构造板块速度(10^{-8}m/s<位移速率<10^{-7}m/s,比传统地震断层的滑移速率(~1 m/s)小了近 8 个数量级)在中地壳压力和温度的条件下产生(Pec et al., 2012b; Marti et al., 2020)。这些非晶态物质与自然界中产生的假玄武玻璃有许多相似之处。地震滑移是否为假玄武玻璃形成的唯一机制是值得重新思考的。有学者认为假玄武玻璃不仅可以在地震断层快速滑移的环境下形成,还可以在中地壳的温度压力条件以接近板块构造速度的慢速滑移条件下产生(Pec et al., 2012b; Aretusini et al., 2017)。

非晶态物质的形成对于理解假玄武玻璃的性质和断层带后续行为具有重要意义。本文第 5 章介绍了熔融成因假玄武玻璃在特定的阶段可以大幅度降低滑动过程中的摩擦阻力和同震断层强度(McKenzie and Brune, 1972; Di Toro et al., 2006; Hung Chiencheng et al., 2019)。最近的研究表明,粉碎、非晶化作用也是断裂带重要的潜在弱化机制,可以促进断裂带的动态弱化和不稳定(Di Toro et al., 2004; Janssen et al., 2010; Pec et al., 2012a, b, 2016; Marti et al., 2020; Dang Jiaxiang and Zhou Yongsheng, 2021)。非晶态物质由于体积膨胀引起的“刚性突变”,使得晶格逐渐失去抵抗剪切应力的能力。而且非晶态物质没有固定的熔点,在“玻璃化转变温度”(Tg)下非晶态物质可以表现出从固态玻璃化到黏性流体行为的流变转化(Marti et al., 2020)。而玻璃化转变温度的典型估计值仅为熔融温度的 2/3 左右(Debenedetti and Stillinger, 2001; Pec et al., 2016)。由于非晶态物质的以上特征,使得非晶态物质在远低于熔融温度时,可以导致断层强度显著降低(Pec et al., 2012a, 2016; Marti et al., 2020)。在中—快速摩擦滑移实验中,石英可在远低于石英熔点温度下产生硅胶(非晶化水合二氧化硅, Di Toro et al., 2004)或非晶态纳米粉末(Rowe et al., 2019),产生的硅胶或非晶态纳米粉末可显著降低剪切强度。实验研究表明,非晶态物质的强度随着温度的升高而降低,当温度升高时(例如在地震断层摩擦加热过程中),非晶态物质可能会对断层岩石的强度产生重大影响(Pec et al., 2012a; Marti et al., 2020)。因此,假玄武玻璃中非晶态物质的存在对断层和剪切带的流变特性和力学响应有着深刻的影响。

7.2 脆—韧性转换带之下的深部地壳是否存在脆性变形

假玄武玻璃是局部高应变变形下岩石发生粉碎—摩擦熔融的产物,通常被认为是地震活动的可靠地质标志。虽然最初被认为主要发生在上地壳,但随着研究的深入,越来越多证据表明在脆—韧性转换带之下也可以形成假玄武玻璃(本文第 4 章)。这些大陆深部地震往往倾向于沿着大陆碰撞带或沿切割“厚”而“冷”的克拉通的断层成核(Campbell et al., 2020; Zhong Xin et al., 2021)。这意味着中上地壳深度的脆性变形和中下地壳甚至地幔深度的晶体塑性变形之间存在着更为复杂的相互作用,对广泛接受的地壳深部岩石强度和力学行为提出了挑战(Orlandini et al., 2019)。

发育在糜棱岩中的假玄武玻璃吸引了地质—地震学家的关注。假玄武玻璃与糜棱岩的形成机制在一定程度上是相互排斥的。摩擦熔融通常与压力有关,是一个快速高应变局部化的脆性过程,而糜棱岩化的特点是矿物发生塑性变形,通常形成于无震状态。温度与深度的同步升高激活了晶体塑性变形机制,岩石在深部的变形通常是塑性流动产生的。如果是不同时代糜棱岩与假玄武玻璃在空间上相互关联,可能是深层次形成的糜棱岩在隆升剥露过程中被中上地壳水平形成的假玄武玻璃所叠加(Passchier, 1982)。但同时期发育假玄武玻璃与糜

棱岩存在明显的悖论,所以这也是为什么几十年来,触发中、深地震的机制一直困扰着地质学家的原因。

虽然同时期的假玄武玻璃与糜棱岩共生困扰着地质学家,但同时也为我们认识地壳深部变形提供了宝贵的窗口。学者们对其进行了大量的理论、实验和实地研究试图解决这一问题,提出了多种理论模型来解释这一现象,总体可以分为两类。第一类观点是认为在一定条件下,中上地壳脆性环境下也可发生塑性变形。如有些学者认为糜棱岩和假玄武玻璃都产生于中上地壳脆性环境,在中上地壳条件下地震滑移过程中摩擦热可以促进围岩发生晶体塑性变形从而导致假玄武玻璃与糜棱岩共生(Kim et al., 2010; Bestmann et al., 2011, 2012)。第二类观点认为这些假玄武玻璃形成于脆韧性转换带之下的韧性变形域。有研究表明,地震(假玄武玻璃)如果要在深度≥25~30Km 的干燥下地壳岩石中发生,要么需要瞬时的高差应力,要么需要局部的弱化机制,因为干燥的下地壳岩石发生摩擦破坏所需的差应力远高于造山带时间尺度上所能承受的应力(Jamtveit et al., 2018; Campbell et al., 2020)。浅层孕震带大地震的余震向深部传播触发的同震高差应力是一种可能的高差应力机制,应力向下地壳的瞬时转移可使地震破裂从较浅部孕震带向下传播(Jamtveit et al., 2018; Papa et al., 2020; Zhong Xin et al., 2021)。关于深部岩石局部弱化机制的讨论有很多,但仍存在激烈的争议,相关的理论模型包括:①热失控或剪切加热(Braeck and Podladchikov, 2007; Kelemen and Hirth, 2007; John et al., 2009),描述了剪切加热和温度依赖性岩石流变学之间的反馈,在这种过程中,黏塑性材料中剪切局部化和晶粒尺寸减小的组合会产生自放大的机械不稳定性从而导致深部韧性域发生局部弱化;②流体诱发的破坏/脱水脆化(Kirby et al., 1996; Hacker et al., 2003; Ferrand et al., 2017),指在岩石中的水合相破裂过程中,由于孔隙流体压力的增加,从而有效应力降低,使岩石从韧性变形转变为脆性变形;③转换断层作用(Kirby, 1987; Green and Burnley, 1989; Schubnel et al., 2013),是指由于体积和/或焓的变化而引起的岩石的力学弱化,但也是由于在转换过程中颗粒尺寸减小而引起的弱化;④变质转变过程引发的不稳定(Incel et al., 2017; Shi Feng et al., 2018);⑤局部反应诱导弱化过程中的应力传递(Austrheim and Boundy, 1994; Scambelluri et al., 2017);⑥先前存在剪切带的重新激活(Reynard et al., 2010)。

脆—韧性转换带之下的深部地壳通常被认为是典型的塑性变形域,但形成于脆—韧性转换带之下甚至上地幔的假玄武玻璃的存在表明深部地壳也存在脆性变形。有些假玄武玻璃成分(矿物组合)结构可以记录同震到震后瞬时压力和温度条件,约束形成环境,揭示深部地壳的变形机制。但由于假玄武玻璃非常容易受到后期地质事件的改变和影响而消失,所以报导的深部假玄武玻璃例子并不多,地球深部岩石的脆性变形机制仍在探索阶段。

7.3　假玄武玻璃形成后对陆壳流变强度的影响

假玄武玻璃形成过程中摩擦熔体的产生与演化对断层强度有着重要的影响,为我们探究发震时断层强度演化提供了一手资料。假玄武玻璃形成后对陆壳的强度的影响同样是值得关注的问题,因为从不稳定性的成核到地震破裂的传播,地壳的强度在很大程度上也控制着地震周期(Passelègue et al., 2021)。

有研究表明,在浅层大陆地壳中(<12 km)产生的假玄武玻璃会“焊接”地震断层,导致断层强度的增加,阻碍沿着同一断层进一步滑动或者重复滑动(Di Toro and Pennacchioni, 2005),导致今后的地震滑动沿着新产生的破裂面或断层面进行(Chester and Chester, 1998; Proctor and Lockner, 2016; Mitchell et al., 2016)。这种观点强调假玄武玻璃形成会增加大陆地壳的强度,并且在今后的演化过程中被“焊接”的断层不会发生弱化。但是也有研究表明相对于花岗质的熔体,玄武岩经摩擦熔融产生的熔体更容易遭受强烈的变形与蚀变,会导致“焊接”作用的减弱,降低断层强度,使随后地震滑动更容易沿着该断层进行(Phillips et al., 2019)。

在深部大陆地壳,假玄武玻璃的形成会对大陆地壳起到弱化作用,影响着大陆地壳随后的构造演化。实验结果表明,在深部地壳条件下(在实验温度 700~900℃,压力 300 MPa),假玄武玻璃系统性的重新激活了晶体塑性变形,主要通过扩散蠕变变形,其强度比母岩弱得多(图 9,在相同实验温度及应变速率下,假玄武玻璃发生塑性变形所需差应力远远小于母岩英云闪长岩),沿断层分布的假玄武玻璃大大降低了地震活动大陆地壳的强度,局部控制了地壳由脆性变形向塑性变形的转变(Passelègue et al., 2021)。在自然界中也观察到含假玄武玻璃岩石重新激活晶体塑性变形(Passchier, 1982; Pennacchioni and Cesare, 1997; Goodwin, 1999;

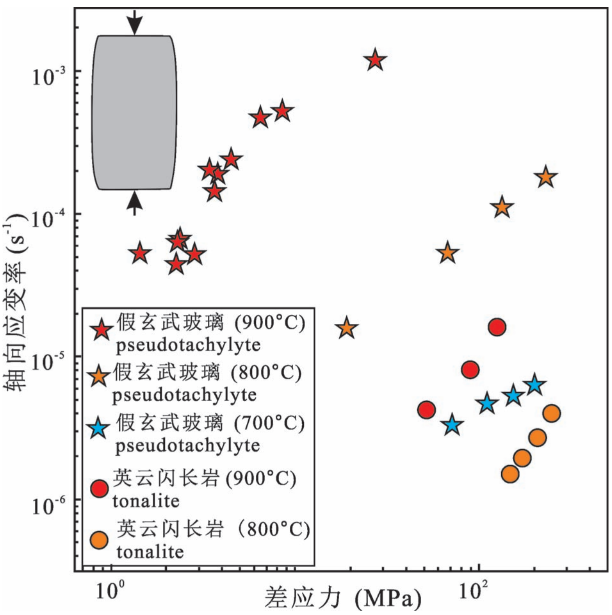

图 9 英云闪长岩和假玄武玻璃进行蠕变实验的力学数据(Passelègue et al., 2021)

Fig. 9 Mechanical data of creep experiments of tonalite and pseudotachylyte (Passelègue et al., 2021)

Menegon et al., 2017)。由于假玄武玻璃的弱化作用,导致含假玄武玻璃岩石的脆—韧性转变发生在比石英和长石更浅的深度上,使得地震生成的假玄武玻璃可能会影响某些反复地震活动断裂带的孕震层厚度,因为在假玄武玻璃发生塑性变形的深度,成熟地壳断层很少发生地震活动(Passelègue et al., 2021)。

8　结论

假玄武玻璃作为古地震的化石记录,是了解地震发展演化的重要窗口,受到国内外学者的广泛关注,取得了一系列重要的研究进展。但受限于假玄武玻璃样品在长期的地质演化过程中不易保存而遭受破坏,关于假玄武玻璃的一些重要科学问题,如脆韧性转换断层之下假玄武玻璃的形成机制、假玄武玻璃形成后对断层强度及地壳强度的控制仍未达成共识。本文通过我们采集的样品初步分析、回顾与总结,得出以下结论:

(1)假玄武玻璃可以形成于地壳不同深度,包括韧性下地壳甚至是上地幔深度。形成于地壳深部与糜棱岩共生的假玄武玻璃表明在脆—韧性转换带之下的传统韧性域也可发生脆性变形。假玄武玻璃的形成类型受控于超碎裂作用或摩擦熔融作用两种主导机制。其中超碎裂成因假玄武玻璃的典型特征为没有发生熔融或生成的熔体量可以忽略不计,基质主要由极细粒的矿物碎屑组成(<1 μm)。

(2)流体(水)在假玄武玻璃形成过程中扮演着多种角色,既有不利因素如降低断层表面的有效正应力、降低剪切强度 τ、促进晶体塑性变形,也有有利因素,如降低单矿物的熔融温度、形成较低黏度的熔体、有利于断层面滑移的启动。断层面上摩擦熔体的润滑与抑制作用是动态变化的。在断层滑动初期起到显著的润滑作用,但当生成熔体的量到达一定程度后,摩擦熔体冷凝固结会起到黏性抑制作用。

(3)假玄武玻璃在天然断层带中很少被发现,其中主要原因是①摩擦熔体的润滑作用导致无法大规模生成假玄武玻璃;②假玄武玻璃在后期地质事件改造,以及风化剥蚀作用下很难完整保存下来。

(4)假玄武玻璃形成对陆壳流变强度也有影响。其中碎裂成因假玄武玻璃中的非晶态物质也可能会降低断层带岩石的强度,对大陆地壳起到弱化作用。

致谢:感谢评审专家对本论文提出宝贵的修改建议,极大地提高了本文的质量。

参　考　文　献　/　References

(The literature whose publishing year followed by a "&" is in Chinese with English abstract; The literature whose publishing year followed by a "#" is in Chinese without English abstract)

戴文浩, 周永胜. 2019. 震后松弛阶段脆塑性转化带的变形: 以红河断裂为例. 地震地质, 41(4): 996~1011.

侯广顺, 夏含峰, 曹高社, 司荣军, 庞绪成, 王珠峰, 何军华. 2013. 嵩山地区假玄武玻璃的发现及其古地震意义. 河南理工大学学报(自然科学版), 32 (2): 151~155.

胡能高, 王志博, 杨家喜. 1995. 贺兰山群变质杂岩中假玄武玻璃的成因. 西安工程学院学报, 17(2): 6~12.

靳立杰, 周汉文, 王继林, 钟增球, 王锦荣. 2014. 豫西双龙剪切带假玄武玻璃的成因及地质意义. 地质科技情报, 33(1): 49~54.

李海兵, 许志琴, 王焕, 张蕾, 何祥丽, 司家亮, 孙知明. 2018. 汶川地震断裂带滑移行为、物理性质及其大地震活动性——来自汶川地震断裂带科学钻探的证据. 地球物理学报, 61(5): 1680~1697.

林爱明, 孙知明, 杨振宇. 2002. 桐柏—大别造山带内与脆性—韧性剪切带共生的假玄武玻璃的发现及意义. 地质学报, 76(3): 373~378.

刘贵, 周永胜. 2012. 长英质岩石的流变学特征及其影响因素. 地震地质, 34(2): 171~189.

刘建民, 董树文, 张家声, 刘晓春, 陈柏林. 2003. 大别造山带东部假玄武玻璃的成因. 地质力学学报, 9(2): 97~105.

刘建民, 董树文, 张家声, 刘晓春, 陈文, 陈柏林. 2004. 大别造山带东部假玄武玻璃及其围岩的 K-Ar 和~(40)Ar-~(39)Ar 年龄及地质意义. 地质学报, 78(3): 374~379.

刘建民，董树文，张家声，刘晓春，陈柏林．2005．大别造山带东部假玄武玻璃的显微构造特征及其意义．地球学报，26(3)：229～234．

刘建民，陈柏林，董树文，赵越，刘晓春．2009．新疆富蕴可可托海—二台断裂带中假玄武玻璃及其围岩的年代学研究．地质论评，55 (4)：581～589．

刘俊来．2017．大陆中部地壳应变局部化与应变弱化．岩石学报，33(6)：1653～1666．

牛露，周永胜，姚文明，邵同宾，马玺，党嘉祥，何昌荣．2018．高温高压条件下彭灌杂岩的强度对汶川地震发震机制的启示．地球物理学报，61(5)：1728～1740．

牛露，周永胜，姚文明，马玺，何昌荣．2021．花岗岩非稳态流变实验．地震地质，43(1)，20～35．

沙绍礼，陈晓林．2013．兰坪河西古元古界雪龙山岩群假玄武玻璃的发现．云南地质，32 (1)：1～4．

邵济安，傅英奇，臧启家，王玉芳．1988．一种含水的构造玻璃．科学通报，(22)：53～56．

史兰斌，林传勇，张小鸥，陈孝德，柏美祥．1997．新疆可可托海二台断裂带假玄武玻璃的基本特征．中国科学，27(2)：137～142．

王焕，李海兵，司家亮，黄尧．2013．汶川地震断裂带结构特征与龙门山隆升的关系．岩石学报，29(6)：2048～2060．

王焕，李海兵，司家亮，孙知明，付小方，刘栋梁，裴军令，李成龙，张佳佳，宋圣荣，郭力伟，Mori J，薛莲，Brodskye E，云锟，龚正．2015．汶川地震断裂作用研究新认识．地球学报，36(3)：257～269．

王焕，李海兵．2019．断裂带中古地震滑动的岩石记录．地球学报，40(1)：135～156．

王历星，焦骞骞，许德如，陈根文，朱昱桦．2019．广东河台金矿假玄武玻璃地球化学和年代学特征及其地质意义．大地构造与成矿学，43(2)：354～366．

杨主恩，应思淮，林传勇，俞理宝．1981．北京密云北石城断裂带的断层岩特征及其地震事件的可能证据．地震地质，3(4)：1～14．

张桂林．1997．假玻状岩研究的新进展．地质科技情报，16(2)：24～28．

张桂林，梁金城．1998．广东河台金矿假玻状岩的形成机制及其与成矿的关系．桂林工学院学报，18(1)：3～9．

张进江，郑亚东．1995．假玄武玻璃及其形成过程和机制综述．地质科技情报，14(4)：22～28．

张蕾，孙知明，李海兵，赵来时，曹勇，叶小舟，王雷振，王焕，何祥丽，韩帅，白明坤，葛成隆，赵越．2017．龙门山构造带 WFSD-2 钻孔岩心磁化率特征及其对大地震活动的响应．地球物理学报，60(1)：225～239．

张蕾，李海兵，孙知明，曹勇，王焕．2019．断裂熔融作用中单质铁的形成及其指示的孕震环境．岩石学报，35 (6)：1875～1891．

张媛媛，周永胜．2012．断层脆塑性转化带的强度与变形机制及其流体和应变速率的影响．地震地质，34(1)：172～194．

周永胜，何昌荣．2009．汶川地震区的流变结构与发震高角度逆断层滑动的力学条件. 地球物理学报,52(2)：474～484．

周永胜，韩亮，靖晨，何昌荣，党嘉祥．2014．龙门山断层脆塑性转化带流变结构与汶川地震孕震机制．地震地质，36(3)：882～893．

周永胜，戴文浩．2021．地壳脆塑性转化带非稳态流变与震后松弛变形机制．地学前缘，28：1～10．https：//doi．org/10．13745/j．esf．sf．2020．9．41

Acosta M，Passelègue F X，Schubnel A，Violay M．2018．Dynamic weakening during earthquakes controlled by fluid thermodynamics．Nature Communications，9(1)：1～9．

Allen A R．1979．Mechanism of frictional fusion in fault zones．Journal of Structural Geology，1(3)：231～243．

Andersen T B，Austrheim H．2006．Fossil earthquakes recorded by pseudotachylytes in mantle peridotite from the Alpine subduction complex of Corsica．Earth and Planetary Science Letters，242 (1～2)：58～72．

Andersen T B，Mair K，Austrheim H，Podladchikov Y Y，Vrijmoed J C．2008．Stress release in exhumed intermediate and deep earthquakes determined from ultramafic pseudotachylyte．Geology，36(12)：995～998．

Aretusini S，Mittempergher S，Plümper O，Spagnuolo E，Gualtieri A F，Di Toro G．2017．Production of nanoparticles during experimental deformation of smectite and implications for seismic slip．Earth and Planetary Science Letters，463：221～231．

Austrheim H，Boundy T M．1994．Pseudotachylytes generated during seismic faulting and eclogitization of the deep crust．Science，265 (5168)：82～83．

Beeler N，Tullis T，Goldsby D．2008．Constitutive relationships and physical basis of fault strength due to flash heating．Journal of Geophysical Research，113(B1)：1～18．

Bestmann M，Pennacchioni G，Frank G，Göken M，de Wall H．2011．Pseudotachylyte in muscovite-bearing quartzite：coseismic friction-induced melting and plastic deformation of quartz．Journal of Structural Geology，33(2)：169～186．

Bestmann M，Pennacchioni G，Nielsen S，Göken M，de Wall H．2012．Deformation and ultrafine dynamic recrystallization of quartz in pseudotachylyte-bearing．Brittle faults：a matter of a few seconds．Journal of Structural Geology，38：21～38．

Bizzarri A，Cocco M．2006a．A thermal pressurization model for the spontaneous dynamic rupture propagation on a three-dimensional fault：1．Methodological approach．Journal of Geophysical Research：Solid Earth，111(B5)：1～22．

Bizzarri A，Cocco M．2006b．A thermal pressurization model for the spontaneous dynamic rupture propagation on a three-dimensional fault：2．Traction evolution and dynamic parameters．Journal of Geophysical Research：Solid Earth，111(B5)：1～18．

Boullier A M，Yeh E C，Boutareaud S，Song S R，Tsai C H．2009．Microscale anatomy of the 1999 Chi-Chi earthquake fault zone．Geochemistry，Geophysics，Geosystems，10(3)：224～234．

Boutareaud S，Calugaru D G，Han R，Fabbri O，Mizoguchi K，Tsutsumi A，Shimamoto T．2008．Clay-clast aggregates：A new textural evidence for seismic fault sliding? Geophysical Research Letters，35 (5)：1～5．

Boutareaud S，Boullier A M，Andréani M，Calugaru D G，Beck P，Song S R，Shimamoto T．2010．Clay clast aggregates in gouges：New textural evidence for seismic faulting．Journal of Geophysical Research，115(B2)：1～15．

Brantut N，Sulem J，Schubnel A．2011．Effect of dehydration reactions on earthquake nucleation：Stable sliding，slow transients，and unstable slip．Journal of Geophysical Research，116(B5)：1～16．

Brantut N，Mitchell T M．2018．Assessing the Efficiency of Thermal Pressurization Using Natural Pseudotachylyte-Bearing Rocks．Geophysical Research Letters，45(18)：9533～9541．

Brantut N．2020．Dilatancy-induced fluid pressure drop during dynamic rupture：Direct experimental evidence and consequences for earthquake dynamics．Earth and Planetary Science Letters，538 (11)：1～10．

Braeck S, Podladchikov Y Y. 2007. Spontaneous thermal runaway as an ultimate failure mechanism of materials. Physical Review Letters, 98(9): 1~4.

Brodsky E E, Kanamori H. 2001. Elastohydrodynamic lubrication of faults. Journal of Geophysical Research, 106(B8): 16357~16374.

Campbell, L R, Menegon, L, Fagereng Å, Pennacchioni G. 2020. Earthquake nucleation in the lower crust by local stress amplification. Nature Communications, 11(1), 1~9.

Chen Xiaofeng, Madden A S E, Reches Z. 2017. Friction evolution of granitic faults: heating controlled transition from powder lubrication to frictional melt. Journal of Geophysical Research: Solid Earth, 122(11): 9275~9289.

Chester F M, Chester J S. 1998. Ultracataclasite structure and friction processes of the Punchbowl fault, San Andreas system, California. Tectonophysics, 295(1~2): 199~221.

Clarke G L, Norman A R. 1993. Generation of pseudotachylite under granulite facies conditions, and its preservation during cooling. Journal of Metamorphic Geology, 11(3): 319~335.

Clerc A, Renard F, Austrheim H, Jamtveit B. 2018. Spatial and size distributions of garnets grown in a pseudotachylyte generated during a lower crust earthquake. Tectonophysics, 733: 159~170.

Clough C T. 1888. The geology of the Cheviot Hills, England and Wales. Geol. Surv. Mem, Sheet 108 NE. 22.

Clough C, Maufe H B, Bailey E B. 1909. The cauldron—subsidence of Glen Coe, and the associated igneous phenomena. Quarterly Journal of the Geological Society, 65(1~4): 611~678.

Collettini C, Chiaraluce L, Pucci S, Barchi M R, Cocco M. 2005. Looking at fault reactivation matching structural geology and seismological data. Journal of Structural Geology, 27(5): 937~942.

Collettini C, Viti C, Tesei T, Mollo S. 2013. Thermal decomposition along natural faults during earthquakes. Geology, 41(8): 927~930.

Cornelio C, Spagnuolo E, Di Toro G, Nielsen S, Violay M. 2019. Mechanical behavior of fluid-lubricated faults. Nature Communications, 10(1): 1~7.

Cowan D S. 1999. Do faults preserve a record of seismic slip? a field geologist's opinion. Journal of Structural Geology, 21(8): 995~1001.

Crovisier J L, Honnorez J, Eberhart J P. 1987. Dissolution of basaltic glass in sea water: mechanism and rate. Geochimica et Cosmochimica Acta, 51(11): 2977~2990.

Dai Wenhao, Zhou Yongsheng. 2019&. Deformation of the brittle—plastic transition zone at the post-seismic relaxation period: a case study of the Red River fault. Seismology and Geology, 41(4): 996~1011.

Dang Jiaxiang, Zhou Yongsheng. 2021. Amorphous materials and clay mineral formation in the coseismic gouge from a surface rupture of the Ms 8. 0 Wenchuan earthquake. Tectonophysics, 818: 1~17.

Debenedetti P G, Stillinger F H. 2001. Supercooled liquids and the glass transition. Nature, 410(6825): 259~267.

Deseta N, Andersen T B, Ashwal L D. 2014a. A weakening mechanism for intermediate-depth seismicity? Detailed petrographic and microtextural observations from blueschist facies pseudotachylytes, Cape Corse, Corsica. Tectonophysics, 610: 138~149.

Deseta N, Ashwal L D, Andersen T B. 2014b. Initiating intermediate-depth earthquakes: Insights from a HP – LT ophiolite from Corsica. Lithos, 206~207: 127~146.

Di Toro G, Goldsby D L, Tullis T E. 2004. Friction falls towards zero in quartz rock as slip velocity approaches seismic rates. Nature, 427(6973): 436~439.

Di Toro G, Pennacchioni G. 2004. Superheated friction-induced melts in zoned pseudotachylytes within the adamello tonalites (Italian southern alps). Journal of Structural Geology, 26 (10): 1783~1801.

Di Toro G, Pennacchioni G. 2005. Fault plane processes and mesoscopic structure of a strongtype seismogenic fault in tonalites (Adamello batholith, Southern Alps): Tectonophysics, 402(1~4): 55~80.

Di Toro G, Hirose T, Nielsen S, Pennacchioni G, Shimamoto T. 2006. Natural and experimental evidence of melt lubrication of faults during earthquakes. Science, 311(5761): 647~649.

Di Toro G, Pennacchioni G, Nielsen S. 2009. Pseudotachylytes and earthquake source mechanics. In: Fukuyama, E. (Ed.), Fault-zone Properties and Earthquake Rupture Dynamics, International Geophysics Series, vol. 94. Elsevier Academic Press, ISBN 978-0-12-374452-4: 87~133.

Dixon J E, Dixon T H. 1989. Vesicles, amygdules and similar structures in fault- generated pseudotachylytes: Comment. Lithos, 20(5): 419~432.

Duxson P, Fernández-Jiménez A, Provis J L, Lukey G C. Palomo A, van Deventer J S J. 2007. Geopolymer technology: the current state of the art. Journal of Materials Science, 42(9): 2917~2933.

Ermanovics I F, Helmstaedt H, Plant A G. 1972. An occurrence of archean pseudotachylite from southeastern manitoba. Canadian Journal of Earth Sciences, 9(3): 257~265.

Evans B W, Cowan D S. 2012. A melt origin for spinifex-textured metaperidotite in the Cerro del Almirez massif, southern Spain. American Journal of Science, 312(9): 967~993.

Fabbri O, Lin A, Totsushige H. 2000. Coeval formation of cataclasite and pseudotachylyte in a Miocene forearc granodiorite, southern Kyushu, Japan. Journal of Structural Geology, 22(8): 1015~1025.

Ferrand T P, Hilairet N, Incel S, Deldicque D, Labrousse L, Gasc J, Schubnel A. 2017. Dehydration-driven stress transfer triggers intermediate-depth earthquakes. Nature Communications, 8: 1~11.

Ferrand T P, Labrousse L, Eloy G, Fabbri O, Hilairet N, Schubnel A. 2018. Energy balance from a Mantle pseudotachylyte, Balmuccia, Italy. Journal of Geophysical Research: Solid Earth, 123(5): 3943~3967.

Ferrand T P, Nielsen S, Labrousse L, Schubnel A. 2021. Scaling seismic fault thickness from the laboratory to the field. Journal of Geophysical Research: Solid Earth, 126(3): 1~20.

Freiman S W. 1984. Effects of chemical environments on slow crack growth in glasses and ceramics. Journal of Geophysical Research: Solid Earth, 89(B6): 4072~4076.

French B M, Koeberl C. 2010. The convincing identification of terrestrial meteorite impact structures: what works, what doesn´t, and why. Earth Science Reviews, 98(1~2): 123~170.

Goldsby D L, Tullis T E. 2002. Low frictional strength of quartz rocks at subseismic slip rates. Geophysical Research Letters, 29(17): 21~25.

Goldsby D L, Tullis T E. 2011. Flash heating leads to low frictional strength of crustal rocks at earthquake slip rates. Science, 334(6053): 216~218.

Goodwin L B. 1999. Controls on pseudotachylyte formation during tectonic exhumation in the south mountains metamorphic core complex, Arizona. Geological Society, London, Special Publications, 154(1): 325~342.

Green H W, Burnley P. 1989. A new self-organizing mechanism for deep-focus earthquakes. Nature, 341(6244): 733~737.

Green H W, Houston H. 1995. The mechanics of deep earthquakes. Annual Review of Earth and Planetary Sciences, 23: 169~213.

Griffith W A, Nielsen S, Di Toro G, Smith S A F. 2010. Rough faults, distributed weakening, and off-fault deformation. Journal of Geophysical Research, 115(B8): 1~22.

Griggs D T. 1967. Hydrolytic weakening of quartz and other silicates. Geophysical Journal of the Royal Astronomical Society, 14(1~4): 19~31.

Hacker B R, Peacock S M, Abers G A, Holloway S D. 2003. Subduction factory 2. Are intermediate-depth earthquakes in subducting slabs linked to metamorphic dehydration reactions? Journal of Geophysical Research: Solid Earth, 108(B1): 1~16.

Han R, Shimamoto T, Hirose T, Ree J H, Ando J i. 2007. Ultralow friction of carbonate faults caused by thermal decomposition. Science, 316(5826): 878~881.

Han R, Hirose T, Shimamoto T. 2010. Strong velocity weakening and powder lubrication of simulated carbonate faults at seismic slip rates. Journal of Geophysical Research, 115(B3): 1~23.

Hawemann F, Mancktelow N S, Pennacchioni G, Wex S, Camacho A. 2019. Weak and slow, strong and fast: how shear zones evolve in a dry continental crust (Musgrave Ranges, Central Australia). Journal of Geophysical Research: Solid Earth, 124(1): 219~240.

Hayward K S, Cox S F, Gerald J F, Slagmolen B, Shaddock D A, Forsyth P, Salmon M L, Hawkins R P. 2016. Mechanical amorphization, flash heating, and frictional melting: dramatic changes to fault surfaces during the first millisecond of earthquake slip. Geology, 44(12): 1043~1046.

Hayward K S, Cox S F. 2017. Melt welding and its role in fault reactivation and localization of fracture damage in seismically active faults. Journal of Geophysical Research: Solid Earth, 122: 9689~9713.

Hemley R J, Jephcoat A P, Mao H K, Ming L C, Manghnani M H. 1988. Pressure-induced amorphization of crystalline silica. Nature, 334 (6177): 52~54.

Henley R W, Ellis A J. 1983. Geothermal systems ancient and modern: a geochemical review. Earth-Science Reviews, 19(1): 1~50.

Hirose T, Shimamoto T. 2003. Fractal dimension of molten surfaces as a possible parameter to infer the slip-weakening distance of the faults from natural pseudotachylyte. Journal of Structural Geology, 25 (10): 1569~1574.

Hirose T, Shimamoto T. 2005. Growth of molten zone as a mechanism of slip weakening of simulated faults in gabbro during frictional melting. Journal of Geophysical Research: Solid Earth, 110(B05): 1~18.

Holland T H. 1900. The charnockite series, a group of Archean hypersthenic rocks in peninsular India. India Geol. Survey Mem, 28(2): 119~249.

Hornby A J, Kendrick J E, Lamb O D, Hirose T, De Angelis S, von Aulock F W, Umakoshi K, Miwa T, Henton De Angelis S, Wadsworth F B, Hess K U, Dingwell D B, Lavalle´e Y. 2015. Spine growth and seismogenic faulting at Mt. Unzen, Japan. Journal of Geophysical Research: Solid Earth, 120(6): 4034~4054.

Hou Guangshun, Xia Hanfeng, Cao Gaoshe, Si Rongjun, Pang Xucheng, Wang Zhufeng, He Junhua. 2013&. Finding of pseudotachylytes in Songshan region and its significance on palaeo-earthquakes. Journal of Henan Polytechnic University (Natural Science), 32 (2): 151~155.

Hu Nenggao, Wang Zhibo, Yang Jiaxi. 1995 #. Genesis of pseudotachylyte in the metamorphic complex of Helanshan group. Journal of Earth Sciences and Environment, 17(2): 6~12.

Hung Chiencheng, Kuo Liwei, Spagnuolo E, Wang Chunchieh, Di Toro G, Wu Wenjie, Dong Jiajyun, Lin Wayne, Sheu Hwoshuenn, Yeh Enchao, Hsieh Peishan. 2019. Grain fragmentation and frictional melting during initial experimental deformation and implications for seismic slip at shallow depths. Journal of Geophysical Research: Solid Earth, 124 (11): 11150~11169.

Hyndman R D, Peacock S M. 2003. Serpentinization of the forearc mantle. Earth and Planetary Science Letters, 212(3~4): 417~432.

Ikesawa E, Sakaguchi A, Kimura G. 2003. Pseudotachylyte from an ancient accretionary complex: evidence for melt generation during seismic slip along a master décollement? Geology, 31(7): 637~640.

Incel S, Hilairet N, Labrousse L, John T, Deldicque D, Ferrand T, Wang Y, Renner J, Morales L, Schubnel A. 2017. Laboratory earthquakes triggered during eclogitization of lawsonite-bearing blueschist. Earth and Planetary Science Letters, 459: 320~331.

Ishikawa T, Tanimizu M, Nagaishi K, Matsuoka J, Tadai O, Sakaguchi M, Song S R. 2008. Coseismic fluid - rock interactions at high temperatures in the Chelungpu fault. Nature Geoscience, 1(10): 679~683.

Jamtveit B, Ben-Zion Y, Renard F, Austrheim H. 2018. Earthquake-induced transformation of the lower crust. Nature, 556(7702): 487~491.

Janssen C, Wirth R, Rybacki E, Naumann R, Kemnitz H, Wenk H R, Dresen G. 2010. Amorphous material in safod core samples (san andreas fault): evidence for crush-origin pseudotachylytes? Geophysical Research Letters, 37(1): 73~78.

Jiang Hehe, Lee C A, Morgan J K, Ross C H. 2015. Geochemistry and thermodynamics of an earthquake: A case study of pseudotachylites within mylonitic granitoid. Earth and Planetary Science Letters, 430: 235~248.

Jin Lijie, Zhou Hanwen, Wang Jilin, Zhong Zengqiu, Wang Jinrong. 2014&. Genesis of pseudotachylites from Shuanglong ductile shear zone and its geological significance. Bulletin of Geological Science and Technology, 33(1): 49~54.

John T, Medvedev S, Rüpke L H, Andersen T B, Podladchikov Y Y, Austrheim H. 2009. Generation of intermediate-depth earthquakes by self-localizing thermal runaway. Nature Geoscience, 2(2): 137~140.

Jung Haemyeong, Green H W, Dobrzhinetskaya L. 2004. Intermediate-depth earthquake faulting by dehydration embrittlement with negative volume change. Nature, 428(6982): 545~549.

Jung Haemyeong, Katayama I, Jiang Zhenting, Hiraga I, Karato S-I. 2006. Effect of water and stress on the lattice-preferred orientation of olivine. Tectonophysics, 421(1~2): 1~22.

Kelemen P B, Hirth G. 2007. A periodic shear-heating mechanism for intermediate-depth earthquakes in the mantle. Nature, 446(7137): 787~90.

Kendrick J E, Lavalle´e Y, Hirose T, Di Toro G, Hornby A J, De Angelis S, Dingwell D B. 2014. Volcanic drumbeat seismicity caused by stick-slip motion and magmatic frictional melting. Nature

Geoscience, 7(6): 438~442.

Kennedy L A, Spray J G. 1992. Frictional melting of sedimentary rock during highspeed diamond drilling: an analytical SEM and TEM investigation. Tectonophysics, 204: 323~337.

Killick A M. 1990. Pseudotachylite generated as a result of a drilling "burn in". Tectonophysics, 171(1~4): 221~227.

Kim J W, Ree J H, Han R, Shimamoto T. 2010. Experimental evidence for the simultaneous formation of pseudotachylyte and mylonite in the brittle regime. Geology, 38(12): 1143~1146.

Kirby S H. 1897. Localized polymorphic phase transformations in high-pressure faults and applications to the physical mechanism of deep earthquakes. Journal of Geophysical Research, 92(B13): 13789.

Kirby S, Engdahl, E R, Denlinger R. 1996. Intermediate-depth intraslab earthquakes and arc volcanism as physical expressions of crustal and uppermost mantle metamorphism in subducting slabs. In: Bebout G E, Scholl D W, Kirby S H, Platt J P (Eds.), Subduction Top to Bottom. Geophysical Monograph. American Geophysical Union, Washington, DC, 195~214.

Kirkpatrick J D, Shipton Z K, Persano C. 2009. Pseudotachylytes: rarely generated, rarely preserved, or rarely reported? Bulletin of the Seismological Society of America, 99(1): 382~388.

Kirkpatrick J D, Shipton Z K. 2009. Geologic evidence for multiple slip weakening mechanisms during seismic slip in crystalline rock. Journal of Geophysical Research, 114(B12): 1~14.

Kirkpatrick J D, Rowe C D. 2013. Disappearing ink: How pseudotachylytes are lost from the rock record. Journal of Structural Geology, 52: 183~198.

Koizumi Y, Otsuki K, Takeuchi A, Nagahama H. 2004. Frictional melting can terminate seismic slips: experimental results of stick-slips. Geophysical Research Letters, 31(21): 1~4.

Kuo Liwei, Song Shengrong, Suppe J, Yeh Enchao. 2016. Fault mirrors in seismically active fault zones: A fossil of small earthquakes at shallow depths. Geophysical Research Letters, 43 (5): 1950~1959.

Kuo Liwei, Di Felice F, Spagnuolo E, Di Toro G, Song Shengrong, Aretusini S, Li Haibing, Suppe J, Si Jialiang, Wen Chengyen. 2017. Fault gouge graphitization as evidence of past seismic slip. Geology, 45(11): 979~982.

Li Haibing, Wang Huan, Xu Zhiqin, Si Jialiang, Pei Junling, Li Tianfu, Huang Yao, Song Shengrong, Kuo Liwei, Sun Zhiming, Chevalier M L, Liu Dongliang. 2013. Characteristics of the fault-related rocks, fault zones and the principal slip zone in the Wenchuan Earthquake Fault Scientific Drilling Project Hole-1 (WFSD-1). Tectonophysics, 584: 23~42.

Li Haibing, Xu Zhiqin, Wang Huan, Zhang Lei, He Xianli, Si Jialiang, Sun Zhiming. 2018&. Fault behavior, Physical properties and seismic activity of the Wenchuan earthquake fault zone: evidences from the Wenchuan earthquake fault scientific drilling project (WFSD). Chinese Journal of Geophysics, 61(5): 1680~1697.

Lin Aiming. 1991. Origin of fault-generated pseudotachylytes. Ph. D. Thesis, Tokyo University, 108.

Lin Aiming. 1994a. Glassy pseudotachylytes from the Fuyun fault zone, Northwest China. Journal of Structural Geology, 16: 71~83.

Lin Aiming. 1994b. Microlite morphology and chemistry in pseudotachylite from the Vredefort Dome, South Africa. N. Jb. Mineral. tachylite, from the Fuyun fault zone, China. The Journal of Geology, 102: 317~329.

Lin Aiming. 1996. Injection veins of crushing-originated pseudotachylyte and fault gouge formed during seismic faulting. Engineering Geology, 43(2~3): 213~224.

Lin Aiming, Shimamoto T. 1998. Selective melting processes as inferred from experimentally generated pseudotachylytes. Journal of Asian Earth Sciences, 16(5~6): 533~545.

Lin Aiming. 1999. Roundness of clasts in pseudotachylytes and cataclastic rocks as an indicator of frictional melting. Journal of Structural Geology, 21(5): 473~478.

Lin Aiming, Sun Zhiming, Yang Zhenyu. 2002&. Pseudotachylytes generated in the Dahezhen brittle—ductile shear zone in the Tongbei—Dabie orogenic belt, China and their significance for seismo-tectonics. Acta Geologica Sinica, 76(3): 373~378.

Lin Aiming. 2008. Fossil Earthquakes: The Formation and Preservation of Pseudotachylytes. Springer Berlin Heidelberg.

Lin Aiming. 2019. Thermal pressurization and fluidization of pulverized cataclastic rocks formed in seismogenic fault zones. Journal of Structural Geology, 125: 278~284.

Liu Gui, Zhou Yongsheng. 2012&. Rheology of felsic rocks and relative influence factors. Seismology and Geology, 34(2): 171~189.

Liu Jianmin, Dong Shuwen, Zhang Jiasheng, Liu Xiaochun, Chen Bailin. 2003&. Origin of pseudotachylites from the eastern Dabieshan orogenic belt. Journal of Geomechanics, 9(2): 97~105.

Liu Jianmin, Dong Shuwen, Zhang Jiasheng, Liu Xiaochun, Chen Wen, Chen Bailin. 2004&. K-Ar and ^{40}Ar-^{39}Ar ages of pseudotachylites and their wall rocks from the Eastern Dabie Mountains and their implications. Acta Geologica Sinica, 78(3): 374~379.

Liu Jianmin, Dong Shuwen, Zhang Jiasheng, Liu Xiaochun, Chen Bailin. 2005&. Microstructure characteristics of pseudotachylites from the Eastern Dabieshan orogenic belt and their tectonic implications. Acta Geoscientica Sinica, 26(3): 229~234.

Liu Jianmin, Chen Bailin, Dong Shuwen, Zhao Yue, Liu Xiaochun. 2009&. Ages of pseudotachylite and its wall rocks from the Keketuohai—Ertai fault zone, Xinjiang, Northwest China. Geological Review, 55 (4): 581~589.

Liu Junlai. 2017&. Strain localization and strain weakening in the continental middle crust. Acta Petrologica Sinica, 33(6): 1653~1666.

Lund M G, Austrheim H. 2003. High-pressure metamorphism and deep-crustal seismicity: evidence from contemporaneous formation of pseudotachylytes and eclogite facies coronas. Tectonophysics, 372 (1~2): 59~83.

MacCulloch J. 1819. Description of the Western Isles of Scotland, Including the Isle of Man, Vol. 1. Edinburgh, Scotland: Constable & Company, 587.

Maddock R H. 1983. Melt origin of fault-generated pseudotachylytes demonstrated by textures. Geology, 11(2): 105~108.

Maddock R H, Grocott J, Van Nes M. 1987. Vesicles, amygdules, and similar structures in fault-generated pseudotachylytes. Lithos, 20 (5): 419~432.

Maddock R H. 1992. Effects of lithology, cataclasis and melting on the composition of fault-generates pseudotachylites in Lewisian gneiss. Scotland. Tectonophysics, 204(3~4): 261~278.

Maggot R, Fabbri O, Fournier M. 2016. Subduction zone intermediate-depth seismicity: Insights from the structural analysis of Alpine high-pressure ophiolitehosted pseudotachylyte (Corsica, France). Journal of Structural Geology, 87: 95~114.

Magott R, Fabbri O. Fournier, M. 2020. Seismically-induced serpentine dehydration as a possible mechanism of water release in subduction zones. Insights from the Alpine Corsica pseudotachylyte-bearing Monte Maggiore ophiolitic unit. Lithos, 362~363 (10): 1~16.

Magloughlin J F. 1989. The nature and significance of pseudotachylite from the Nason terrane, North Cascade Moun tains, Washington. Journal of Structural Geology, 11: 907~917.

Magloughlin J F. 1992. Microstructural and chemical changes associated with cataclasis and frictional melting at shallow crustal levels: The cataclasite—pseudotachylyte connection. Tectonophysics, 204(3~4): 243~260.

Magloughlin J F, Spray J G. 1992. Frictional melting processes and products in geological materials: introduction and discussion. Tectonophysics, 204(3~4): 197~204.

Magloughlin J F. 2005. Immiscible sulfide droplets in pseudotachylyte: Evidence for high temperature (<1200°C) melts. Tectonophysics, 402(1~4): 81~91.

Martini J E J. 1992. The metamorphic history of the vredefort dome at approximately 2 Ga as revealed by coesite—stishovite-bearing pseudotachylites. Journal of Metamorphiee Gology, 10: 517~527.

Marti S, Stünitz H, Heilbronner R, Plümper O. 2020. Amorphous material in experimentally deformed mafic rock and its temperature dependence: Implications for fault rheology during aseismic creep and seismic rupture. Journal of Structural Geology, 138: 104081.

McKenzie D, Brune J N. 1972. Melting on fault planes during large earthquakes. Geophysical Journal International, 29(1): 65~78.

Melosh H J. 2005. The mechanics of pseudotachylite formation in impact events. In: Koeberl C, Henkel H (Eds.), Impact Tectonics. Impact Studies Series, Springer, Berlin, Heidelberg, 55~80.

Menegon L, Pennacchioni G, Malaspina N, Harris K, Wood E. 2017. Earthquakes as precursors of ductile shear zones in the dry and strong lower crust. Geochemistry, Geophysics, Geosystems, 18: 4356~4374.

Mitchell T M, Toy V, Di Toro G, Renner J, Sibson R H. 2016. Fault welding by pseudotachylyte formation. Geology, 44(12): 1059~1062.

Moecher D P, Steltenpohl M G. 2011. Petrological evidence for co-seismic slip in extending middle - lower continental crust: Heier´s zone of pseudotachylyte, north Norway. Geological Society, London, Special Publications, 359(1): 169~186.

Morin G P, Vigier N, Verney-Carron A. 2015. Enhanced dissolution of basaltic glass in brackish waters: impact on biogeochemical cycles. Earth and Planetary Science Letters, 417: 1~8.

Morishita T. 1998. Possible pseudotachylyte from the Horoman peridotite complex of the Hidaka belt, Hokkaido, northern Japan. Journal of Geological Society of Japan, 104(1): 18~23.

Niemeijer A R, Di Toro G, Nielsen S, Di Felice F. 2011. Frictional melting of gabbro under extreme experimental conditions of normal stress, acceleration and sliding velocity. Journal of Geophysical Research: Solid Earth, 116(B7): 1~18.

Niu Lu, Zhou Yongsheng, Yao Wenming, Shao Tongbin, Ma Xi, Dang JiaXiang, He Changrong. 2018&. Experiments on the strength of Pengguan Complex under high temperature and high pressure and high pressure and its implication to seismogenic mechanism of the Wenchuan earthquake. Chinese Journal of Geophysics, 61(5): 1728~1740.

Niu Lu, Zhou Yongsheng, Yao Wenming, Ma Xi, He Changrong. 2021&. An experimental study on the transient creep of granite. Seismology and Geology, 43(1): 20~35.

Obata M, Karato S. 1995. Ultramafic pseudotachylite from the Balmuccia peridotite, Ivrea—Verbano zone, northern Italy. Tectonophysics, 242(3~4): 313~328.

O' Hara K D. 1992. Major- and trace-element constraints on the petrogenesis of a fault-related pseudotachylyte, west ern Blue Ridge province, North Carolina. Tectonophysics, 204: 279~288.

O'Hara K, Sharp Z. 2001. Chemical and oxygen isotope composition of natural and artificial pseudotachylyte: role of water during frictional fusion. Earth and Planetary Science Letters, 184(2): 393~406.

Oohashi K, Hirose T, Shimamoto T. 2011. Shear-induced graphitization of carbonaceous materials during seismic fault motion: Experiments and possible implications for fault mechanics. Journal of Structural Geology, 33(6): 1122~1134.

Orlandini O F, Mahan K H, Williams M J, Regan S P, Mueller K J. 2019. Evidence for deep crustal seismic rupture in a granulite-facies, intraplate, strike-slip shear zone, northern Saskatchewan, Canada. Geological Society of America Bulletin, 131(3~4): 403~425.

Otsuki K, Monzawa N, Nagase T. 2003. Fluidization and melting of fault gouge during seismic slip: Identification in the Nojima fault zone and implications for focal earthquake mechanisms. Journal of Geophysical Research: Solid Earth, 108(B4): 1~18.

Ozawa K, Takizawa S. 2007. Amorphous material formed by the mechanochemical effect in natural pseudotachylyte of crushing origin: a case study of the Iida Matsukawa Fault, Nagano Prefecture, Central Japan. Journal of Structural Geology, 29(11): 1855~1869.

Papa S, Pennacchioni G, Menegon L, Thielmann M. 2020. High-stress creep preceding coseismic rupturing in amphibolite-facies ultramylonites. Earth and Planetary Science Letters, 541(11): 1~13.

Papa S, Spagnuolo E, Toro G D, Cavallo A, Camacho A, Pennacchioni G. 2021. Selective clast survival in an experimentally-produced pseudotachylyte. Journal of Structural Geology, 147(4): 1~11.

Passchier C W. 1982. Pseudotachylyte and the development of ultramylonite bands in the Saint—Barthelemy Massif, French Pyrenees. Journal of Structural Geology, 4(1): 69~79.

Passelègue F X, Tielke J, Mecklenburgh J, Violay M, Deldicque D, Di Toro G. 2021. Experimental plastic reactivation of pseudotachylyte-filled shear zones. Geophysical Research Letters, 48(5): 1~9.

Pec M, Stünitz H, Heilbronner R. 2012a. Semi-brittle deformation of granitoid gouges in shear experiments at elevated pressures and temperatures. Journal of Structural Geology, 38: 200~221.

Pec M, Stünitz H, Heilbronner R, Drury M, de Capitani C. 2012b. Origin of pseudotachylites in slow creep experiments. Earth and Planetary Science Letters, 355~356: 299~310.

Pec M, Stünitz H, Heilbronner R, Drury M. 2016. Semi-brittle flow of granitoid fault rocks in experiments. Journal of Geophysical Research: Solid Earth, 121(3): 1677~1705.

Pennacchioni G, Cesare B. 1997. Ductile—brittle transition in pre-alpine amphibolite facies mylonites during evolution from water-present to water-deficient conditions (Mont Mary Nappe, Italian Western Alps). Journal of Metamorphic Geology, 15(6): 777~791.

Phillips N J, Rowe C D, Ujiie K. 2019. For how long are pseudotachylytes strong? Rapid alteration of basalt-hosted pseudotachylytes from a shallow subduction complex. Earth and Planetary Science Letters, 518: 108~115.

Philpotts A R. 1964. Origin of Pseudotachylites. American Journal of Science, 262: 1008~1035.

Piccardo G B, Ranalli G, Guarnieri L. 2010. Seismogenic shear zones in the lithospheric mantle: ultramafic pseudotachylytes in the Lanzo Peridotite (Western Alps, NW Italy). Journal of Petrology, 51(1－2): 81~100.

Proctor B, Lockner D A. 2016. Pseudotachylyte increases the post-slip strength of faults. Geology, 44 (12): 1003~1006.

Rahier H, Van Mele B, Biesemans M, Wastiels J, Wu X. 1996. Low-temperature synthesized aluminosilicate glasses. Journal of Materials Science, 31(1): 71~79.

Rahier H, Simons W, Van Mele B, Biesemans M. 1997. Low-temperature synthesized aluminosilicate glasses: part iii influence of the composition of the silicate solution on production, structure and properties. Journal of Materials Science, 32(9): 2237~2247.

Ray S K. 1999. Transformation of cataclastically deformed rocks to pseudotachylyte by pervasion of frictional melt: inference from clast-size analysis. Tectonophysics, 301(3~4): 283~304.

Reches Z, Lockner D. 2010. Fault weakening and earthquake instability by powder lubrication. Nature, 467(7314): 452~455.

Reimold W U. 1995. Pseudotachylite in impact structures-generation by friction melting and shock brecciation: A review and discussion. Earth Science Reviews, 39 (3~4): 247~265.

Reimold W U, Hauser N, Hansen B T, Thirlwall M, Hoffmann M. 2017. The impact pseudotachylitic breccia controversy: Insights from first isotope analysis of Vredefort impact-generated melt rocks. Geochimica et Cosmochimica Acta, 214: 266~281.

Reynard B, Nakajima J, Kawakatsu H. 2010. Earthquakes and plastic deformation of anhydrous slab mantle in double Wadati-Benioff zones. Geophysical Research Letters, 37(24): 1~6.

Rice J R. 2006. Heating and weakening of faults during earthquake slip. Journal of Geophysical Research, 111(B5): 1~29.

Rowe C D, Moore J C, Meneghini F, McKeirnan A W. 2005. Large-scale pseudotachylytes and fluidized cataclasites from an ancient subduction thrust fault. Geology, 33(12): 937~940.

Rowe C D, Kirkpatrick J D, Brodsky E E. 2012. Fault rock injections record paleo-earthquakes, Earth and Planetary Science Letters, 335~336: 154~166.

Rowe C D, Griffith W A. 2015. Do faults preserve a record of seismic slip: A second opinion. Journal of Structural Geology, 78: 1~26.

Rowe C D, Lamothe K, Rempe M, Andrews M, Mitchell T M, Di Toro G, White J C, Aretusini S. 2019. Earthquake lubrication and healing explained by amorphous nanosilica. Nature Communications, 10(1): 320: 1~11.

Scambelluri M, Pennacchioni G, Gilio M, Bestmann M, Plümber O, Nestola F. 2017. Fossil intermediate-depth earthquakes in subducting slabs linked to differential stress release. Nature Geoscience, 10(12): 960~966.

Scholz C H, Sykes L R, Aggarwal Y P. 1973. Earthquake prediction: A physical basis. Science, 181(4102): 803~810.

Schubnel A, Brunet F, Hilairet N, Gasc J, Wang Y, Green H W. 2013. Deep-focus earthquake analogs recorded at high pressure and temperature in the laboratory. Science, 341(6152): 1377~1380.

Shand S J. 1916. The pseudotachylyte of Parijs (Orange Free State), and its relation to "trap—shotten gneiss" and "flinty crush-rock." Quarterly Journal of the Geological Society, 72(1~4): 198~221.

Sha Shaoli, Chen Xiaolin. 2013#. The discovery of pseudotachylyte in Hexi palaeoproterozoic Xuelongshan eock group, Lanping. Yunnan Geology, 32 (1): 1~4.

Shao Jian, Fu Yingqi, Zang Qijia, Wang Yufang. 1988#. An aqueous structural glass. Chinese Science Bulletin, (22): 53~56.

Shi Feng, Wang Yanbin, Yu Tony, Zhu Lupei, Zhang Junfeng, Wen Jianguo, Gasc J, Incel S, Schubnel A, Li Ziyu, Chen Tao, Liu Wenlong, Prakapenka V, Jin Zhenmin. 2018. Lower-crustal earthquakes in southern Tibet are linked to eclogitization of dry metastable granulite. Nature Communication, 9(1): 1~13.

Shi Lanbin, Lin Chuanyong, Zhang xiaoou, Chen Xiaode, Bai Meixiang. 1997#. Basic characteristics of pseudotachylyte in Keketuohai—Ertai fault zone, Xinjiang. Science in China (Series D), 27(2): 137~142.

Sibson R H. 1973. Interactions between temperature and pore-fluid pressure during earthquake faulting and a mechanism for partial or total stress relief. Nature Physical Science, 243(126): 66~68.

Sibson R H. 1975. Generation of Pseudotachylyte by Ancient Seismic Faulting. Geophysical Journal of the Royal Astronomical Society, 43 (3): 775~794.

Sibson R H. 1977. Fault rocks and fault mechanisms. Journal of the Geological Society, 133(3): 191~213.

Sibson R H. 1980. Transient discontinuities in ductile shear zones. Journal of Structural Geology, 2(1): 165~174.

Sibson R H. 1986. Brecciation processes in fault zones: inferences from earthquake rupturing. Pure & Applied Geophysics, 124(1): 159~175.

Sibson R H. 1994. Crustal Stress, Faulting and Fluid Flow. Geological Society, London, Special Publications, 78(1): 69~84.

Sibson R H, Toy V G. 2006. The habitat of fault-generated pseudotachylyte: presence vs. absence of friction-melt// Washington, D. C: American Geophysical Union, 153~166.

Song Wonjoon, Johnson S E, Gerbi C C. 2020. Quartz fluid inclusion abundance and off-fault damage in a deeply exhumed, strike-slip, seismogenic fault. Journal of Structural Geology, 139: 1~20.

Spray J G. 1987. Artificial generation of pseudotachylyte using frictional welding apparatus: simulation of melting on a fault plane. Journal of Structural Geology, 9(1): 44~60.

Spray J G. 1992. A physical basis for the frictional melting of some rock-forming minerals. Tectonophysics, 204(3~4): 205~221.

Spray J G. 1995. Pseudotachylyte controversy: Fact or friction? Geology, 23(12): 1119~1122.

Spray J G. 2010. Frictional melting processes in planetary materials: From hypervelocity impact to earthquakes. Annual Review of Earth and Planetary Sciences, 38(1): 221~254.

Swanson M T. 1992. Fault structure, wear mechanism and rupture process in pseudotachylite generation. In Magloughlin J F, Spray J G eds. Frictional Melting Process es and Products in Geological Materials. Tectonophysics, 204: 223~242.

Tomioka N, Kondo H, Kunikata A, Nagai T. 2010. Pressure-induced amorphization of albitic plagioclase in an externally heated diamond anvil cell. Geophysical Research Letters, 37(21): 1~5.

Toyoshima T. 1990. Pseudotachylite from the Main Zone of the Hidaka metamorphic belt, Hokkaido, northern Japan. Journal of Metamorphic Geology, 8(5): 507~523.

Tsutsumi A, Shimamoto T. 1997. High-velocity frictional properties of gabbro. Geophysical Research Letters, 24(6): 699~702.

Ueda T, Obata M, Di Toro G, Kanagawa K, Ozawa K. 2008. Mantle earthquakes frozen in mylonitized ultramafic pseudotachylytes of spinel—lherzolite facies. Geology, 36(8): 607~610.

Ueda T, Obata M, Ozawa K, Shimizu I. 2020. The ductile-to-brittle transition recorded in the Balmuccia peridotite body, Italy: Ambient temperature for the onset of seismic rupture in mantle rocks. Journal of Geophysical Research: Solid Earth, 125(2): 1~27.

Ujiie K, Kimura G. 2014. Earthquake faulting in subduction zones: insights from fault rocks in accretionary prisms. Progress in Earth and Planetary Science, 1(1~7): 1~30.

Verberne B A, Plumper O, Matthijs de Winter D A, Spiers C J. 2014. Superplastic nanofibrous slip zones control seismogenic fault friction. Science, 346(6215): 1342~1344.

Viesca R C, Garagash D I. 2015. Ubiquitous weakening of faults due to thermal pressurization. Nature Geoscience, 8(11): 875~879.

Wallace P A, Sarah H, Hornby A J, Kendrick J E, Clesham S, Aulock F V. 2019. Frictional melt homogenisation during fault slip: Geochemical, textural and rheological fingerprints. Geochimica et Cosmochimica Acta, 255: 265~288.

Wang Huan, Li Haibing, Si Jialiang, Huang Yao. 2013&. The relationship between the internal structure of the Wenchuan earthquake fault zone and the uplift of the Longmenshan. Acta Petrologica Sinica, 29(6): 2048~2060.

Wang Huan, Li Haibing, Christoph J, Sun Zhiming, Si Jialiang. 2015. Multiple generations of pseudotachylyte in the Wenchuan fault zone and their implications for coseismic weakening. Journal of Structural Geology, 74: 159~171.

Wang Huan, Li Haibing, Si Jialiang, Sun Zhiming, Fu Xiaofang, Liu Dongliang, Pei Junling, Li Chenglong, Zhang Jiajia, Song Shengrong, Guo Liwei, Mori J, Xue Lian, Brodskye E, Yun Kun, Gong Zheng. 2015&. Progress in the Study of the Wenchuan Earthquake faulting. Acta Geoscientica Sinica, 36(3): 257~269.

Wang Huan, Li Haibing, Si Jialiang, Zhang Lei, Sun Zhiming. 2019. Geochemical features of the pseudotachylytes in the Longmen Shan thrust belt, eastern Tibet. Quaternary International, 514: 173~185.

Wang Huan, Li Haibing. 2019&. Seismic slip records preserved in fault rocks. Acta Geoscientica Sinica, 40(1): 135~156.

Wang Lixing, Jiao Qianqian, Xu Deru, Chen Genwen, Zhu Yuhua. 2019&. Geochronology, geochemistry and geological significance of pseudotachylites in Hetai Goldfield, Guangdong Province. Geotectonica et Metallogenia, 43(2): 354~366.

Weiss L E, Wenk H R. 1983. Experimentally produced pseudotachylite-like veins in gabbro. Tectonophysics, 96(3~4): 299~310.

Wenk H R. 1978. Are pseudotachylytes products of fracture or fusion? Geology, 6(8): 507~511.

Wenk H R, Weiss L E. 1982. Al-rich pyroxene in pseudotachylite: an indication of high pressures and temperatures? Tectonophysics, 84: 329~341.

White J C. 1996. Transient discontinuities revisited: pseudotachylyte, plastic instability and the influence of low pore fluid pressure on deformation processes in the mid-crust. Journal of Structural Geology, 18(12): 1471~1486.

Wolf D, Okamoto P R, Yip S, Lutsko J F, Kluge M. 1990. Thermodynamic parallels between solid-state amorphization and melting. Journal of Materials Research, 5(2): 286~301.

Yamashita T, Schubnel A. 2016. Slow slip generated by dehydration reaction coupled with slip-induced dilatancy and thermal pressurization. Journal of Seismology, 20(4): 1217~1234.

Yang Zhuen, Ying Sihuai, Lin Chuanyong, Yu Libao. 1981#. Fault rock characteristics and possible evidence of seismic events of beishicheng fault zone in Miyun, Beijing. Seismology and Geology, 3(4): 1~14.

Yip S, Phillpot S R, Wolf D. 2005. Crystal Disordering in Melting and Amorphization. Handbook of Materials Modeling: 2009~2023.

Yund R A, Blanpied M L, Tullis T E, Weeks J D. 1990. Amorphous material in high strain experimental fault gouges. Journal of Geophysical Research: Solid Earth, 95(B10): 15589~15602.

Zhang Guilin. 1997&. New advancement of study on pseudotachylytes. Bulletin of Geological Science and Technology, 16(2): 24~28.

Zhang Guilin, Liang Jincheng. 1998&. The formation mechanism of pseudotachylyte and its relation to mineralization in Hetai gold mine, Guangdong. Journal of Guilin University of Technology, 18(1): 3~9.

Zhang Jinjiang, Zheng Yadong. 1995&. A general survey of pseudotachylyte and its formation process and mechanism. Bulletin of Geological Science and Technology, 14(4): 22~28.

Zhang Lei, Sun Zhiming, Li Haibing, Zhao Laishi, Cao Yong, Ye Xiaozhou, Wang Leizhen, Wang Huan, He Xiangli, Han Shuai, Bai Mingkun, Ge Chenglong, Zhao Yue. 2017&. Magnetic susceptibility of WFSD-2 borehole cores from the Longmenshan thrust belt and its implications for great seismic activity. Chinese Journal of Geophysics, 60(1): 225~239.

Zhang Lei, Li Haibing, Sun Zhiming, Cao Yong, Wang Huan. 2019&. Metallic iron formed by melting and its seismogenic setting indication. Acta Petrologica Sinica, 35 (6): 1875~1891.

Zhang Lei, Li Haibing, Sun Zhiming, Cao Yong, Wang Huan. 2021. Microstructural evolution of pseudotachylyte-bearing rocks during increasing temperatures: Evidence from rock-heating experiments. Journal of Structural Geology, 104398(149): 1~14.

Zhang Yuanyuan, Zhou Yongsheng. 2012&. The strength and deformation mechanisms of brittle—plastic transition zone, and the effects of strain rate andfluids. Seismology and Geology, 34(1): 172~194.

Zheng Yong, Li Haibing, Sun Zhiming, Wang Huan, Zhang Jiajia, Li Chenglong, Cao Yong. 2016. New geochronology constraints on timing and depth of the ancient earthquakes along the Longmen Shan fault belt, eastern Tibet. Tectonics, 35(12): 2781~2806.

Zhong Xin, Petley-Ragan A J, Incel S H M, Dabrowski M, Jamtveit B. 2021. Lower crustal earthquake associated with highly pressurized frictional melts. Nature Geoscience, 14: 519~525.

Zhou Yongsheng, He Changrong. 2009&. The rheological structures of crust and mechanics of high angle reverse fault slip for Wenchuan MS 8.0 earthquake. Chinese Journal of Geophysics, 52(2): 474~484.

Zhou Yongsheng, Han Liang, Jing Chen, He Changrong, Dang Jiaxiang. 2014&. The rheological structures of brittle—plastic transition in longmenshan fault zone and seismogenic mechanism of wenchuan earthquake. Seismology and Geology, 36(3): 882~893.

Zhou Yongsheng, Dai Wenhao. 2021&. Transient creep during crustal brittle—plastic transition and deformation mechanism of Postseismic relaxation. Earth Science Frontiers, 28: 1~10.

Formation mechanisms of pseudotachylyte in fault zone and significance of unsteady rheology

LI Wenyuan, CAO Shuyun

State Key Laboratory of Geological Processes and Mineral Resources, School of Earth Sciences, China University of Geosciences, Wuhan, 430074

Abstract: Tectonic pseudotachylyte is rare glassy or aphanitic rock, which often occurs in fault zones. It is considered as a fossil record of rapid sliding of paleo-earthquakes. Formation of pseudotachylyte can effectively reduce the friction strength of rock or fault. Therefore, the study of pseudotachylyte is of great significance to understand the fault deformation and seismic genetic mechanism in deep crust. Although many studies have carried on pseudotachylyte, due to the rare occurring of natural pseudotachylyte and its complexity formation process, there are still many disputes and key scientific problems to be solved such as the structural characteristics, formation environment, and genetic mechanism of pseudotachylyte. The pseudotachylyte can be developed in different depth ranges of continental lithosphere, that is, a ductile deformation domain dominated by mylonite in the middle to lower crust and even the upper mantle (> 60 km), or a brittle deformation domain dominated by cataclastic rock in the middle to upper crust (< 12 km). More evidence shows that the pseudotachylyte form in the brittle—ductile transition domain of the fault zone, which is directly related to shallow seismic activity. It also means that there is a more complex coupling relationship between the brittle deformation of the middle—upper crust and the plastic deformation of the middle—lower crust. There is a long debate on the formation mechanisms of pseudotachylyte, which is caused by friction heating on the fault plane or only the rock comminution on the fault plane. It is believed that the dry environment is conducive to the formation of pseudotachylyte. Because the existence of fluid will reduce the effective normal stress of fault plane, which is not conducive to the accumulation of heat and the progress of friction melting. However, another view is suggested that the presence of fluid can reduce the melting temperature of minerals, which is conducive to fault friction melting and the formation of pseudotachylyte. This paper summarizes the formation mechanism, formation depth, fluid influence, influence on fault strength after formation, and preservation and failure mechanism of pseudotachylyte. Then it further to discuss the origin of amorphous materials in pseudotachylyte, the deformation mechanism of rocks under brittle—ductile transition zone, and the influence on continental crust strength and significance of unsteady rheology.

Keywords: Pseudotachylyte; comminution mechanism; friction melting; fault weakening and strengthening; earthquake; fluid activity

Acknowledgements: Thank the review experts for their valuable suggestions on the revision of this paper, which greatly improves the quality of this paper. This work is financially mainly jointly supported by the National Natural Science Foundations of China (Nos. 41972220, 41722207) and National Key Research and Development Program (No. SQ2017YFSF040030)

First author: LI Wenyuan, male, born in 1996, doctoral student, mainly engaged in structural geology; Email: Wenyuanli@cug.edu.cn

Corresponding author: CAO Shuyun, female, born in 1978, professor, mainly engaged in regional structural geology and microstructure; Email: shuyun.cao@cug.edu.cn

Manuscript received on: 2021-09-06; Accepted on: 2022-01-04; Network published on: 2022-01-20

Doi: 10.16509/j.georeview.2022.01.081 **Edited by**: LIU Zhiqiang